Chapter 4

ZrO_2 : RE –Polyacrylic acid Nanocomposites

4.1 Introduction:

Synthesis as well as characterization of ZrO_2:RE - polyacrylicacid nanocomposites are discussed in this part. This chapter gives the process of synthesizing rare earth RE (Ce, Dy, Er, Eu, Pr, Tb, Tm) doped ZrO_2 nano crystallites by hydrothermal technique with 0.1mol% & 0.2mol% doping concentration of rare earth elements. Fourteen such samples were synthesized and incorporated with polyacrylicacid (PAA) to develop thin films of polyacrylicacid- ZrO_2:RE nanocomposites. The samples were characterized by various techniques, which are described in Chapter 2.

4.2 Synthesis of Samples:

Precursors

Zirconyl Nitrate	$ZrO(NO_3)_2.H_2O$
Liquor Ammonia	NH_4OH
Cerium Nitrate Hexa Hydrate	$Ce(NO_3)_3.6H_2O$
Dysprosium Nitrate Hexa Hydrate	$Dy(NO_3)_3.6H_2O$
Erbium Nitrate Hexa Hydrate	$Er(NO_3)_3.6H_2O$
Europium Nitrate Hexa Hydrate	$Eu(NO_3)_3.6H_2O$
Praseodymium Nitrate Hexa Hydrate	$Pr(NO_3)_3.6H_2O$
Terbium Nitrate Hexa Hydrate	$Tb(NO_3)_3.6H_2O$
Thulium Nitrate Hexa Hydrate	$Tm(NO_3)_3.6H_2O$
De-Ionized Water	H_2O
Acrylicacid (Monomer)	$CH_2CHCOOH$
Potassium Persulfate (KPS)	$K_2S_2O_8$

All these chemicals are of analytical grade and used as received.

Preparation of RE (Ce, Dy, Er, Eu, Pr, Tb, Tm) doped ZrO_2 nanoparticles

RE (Ce, Dy, Er, Eu, Pr, Tb, Tm) doped ZrO_2 nanoparticles with 0.1 mol% & 0.2 mol% doping concentration of rare earth elements (for 20 mmol) were prepared by hydrothermal method. Fourteen such samples were synthesized and the process is shown in a flowchart given below.

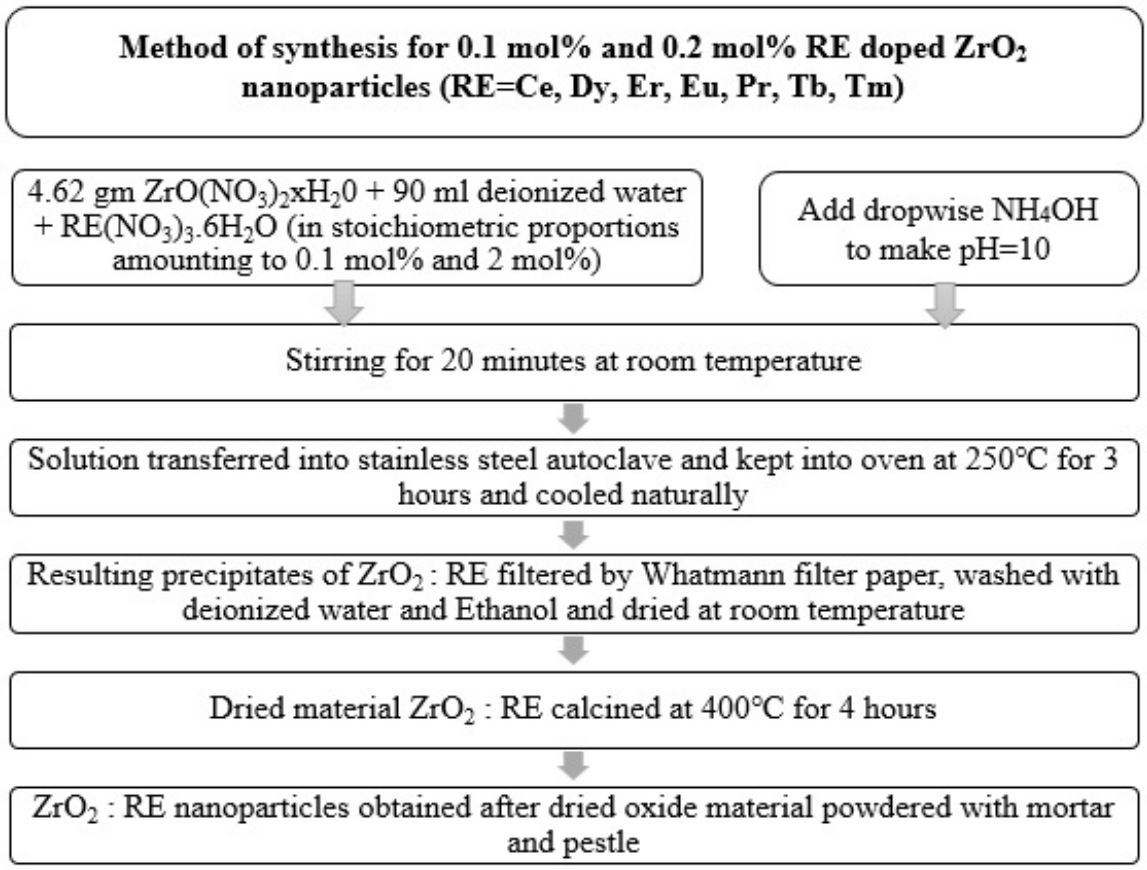

Preparation of polyacrylicacid- ZrO_2:RE nanocomposites

Synthesized [RE (Ce, Dy, Er, Eu, Pr, Tb, Tm) doped ZrO_2] samples were incorporated with polyacrylicacid (PAA) with 1 mol% & 2 mol% to develop thin films of material. The process is shown in the flowchart given below. Fourteen samples were prepared using doctor blade method with uniform thickness for two different concentrations of the seven-doped samples.

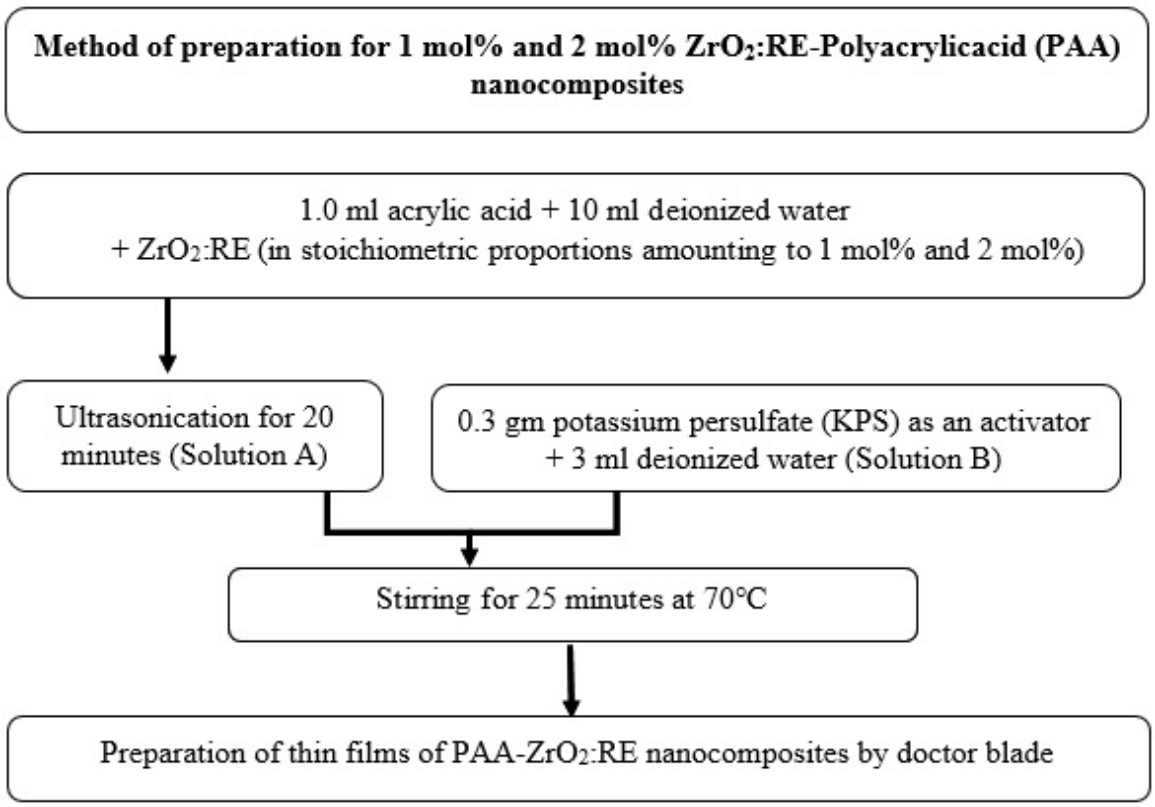

Samples of the prepared nanocomposites are as under.

Table 4.1: Samples labelled and their descriptions

Sample Label	Description
ZCe1	0.1 mol% Ce doped ZrO_2 nanoparticles
ZDy1	0.1 mol% Dy doped ZrO_2 nanoparticles
ZEr1	0.1 mol% Er doped ZrO_2 nanoparticles
ZEu1	0.1 mol% Eu doped ZrO_2 nanoparticles
ZPr1	0.1 mol% Pr doped ZrO_2 nanoparticles
ZTb1	0.1 mol% Tb doped ZrO_2 nanoparticles
ZTm1	0.1 mol% Tm doped ZrO_2 nanoparticles
ZCe2	0.2 mol% Ce doped ZrO_2 nanoparticles
ZDy2	0.2 mol% Dy doped ZrO_2 nanoparticles
ZEr2	0.2 mol% Er doped ZrO_2 nanoparticles
ZEu2	0.2 mol% Eu doped ZrO_2 nanoparticles
ZPr2	0.2 mol% Pr doped ZrO_2 nanoparticles
ZTb2	0.2 mol% Tb doped ZrO_2 nanoparticles
ZTm2	0.2 mol% Tm doped ZrO_2 nanoparticles
PZCe1	1 mol% ZrO_2:Ce-PAA nanocomposites
PZDy1	1 mol% ZrO_2:Dy-PAA nanocomposites
PZEr1	1 mol% ZrO_2:Er-PAA nanocomposites
PZEu1	1 mol% ZrO_2:Eu-PAA nanocomposites
PZPr1	1 mol% ZrO_2:Pr-PAA nanocomposites
PZTb1	1 mol% ZrO_2:Tb-PAA nanocomposites
PZTm1	1 mol% ZrO_2:Tm-PAA nanocomposites
PZCe2	2 mol% ZrO_2:Ce-PAA nanocomposites
PZDy2	2 mol% ZrO_2:Dy-PAA nanocomposites
PZEr2	2 mol% ZrO_2:Er-PAA nanocomposites
PZEu2	2 mol% ZrO_2:Eu-PAA nanocomposites
PZPr2	2 mol% ZrO_2:Pr-PAA nanocomposites
PZTb2	2 mol% ZrO_2:Tb-PAA nanocomposites
PZTm2	2 mol% ZrO_2:Tm-PAA nanocomposites

4.3 Characterization:

X-Ray Diffraction (XRD), Energy Dispersive X-ray Spectroscopy (EDS) and Particle Size Analyser (DLS) studied the structural and elemental properties of the powder samples. Fourier Transformation Infra-Red Spectroscopy (FTIR) studies the functional groups in the samples.

4.3.1 Structural and Elemental properties of powder nanoparticles (X-Ray Diffraction, Energy Dispersive X-ray Spectroscopy and Particle Size Analyzer)

X-ray powder diffraction of the powder samples was carried out on a GNR APD 2000 PRO X-ray Diffractometer. The 2θ range was taken from 10° to 80° in scan mode with step increment of 0.020° at room temperature.

The Energy Dispersive X-ray Spectroscopy (EDS) of the samples was carried out on a spectrometer attached to the Scanning Electron Microscope JEOL make JSM 5810 LV. The distribution of the hydrodynamic diameters of the nanoparticles were determined using a Malvern Nano ZS particle size analyzer by Dynamic Light Scattering (DLS) technique.

Figure 4.1(a) shows the XRD pattern of 0.1 mol% Ce doped ZrO_2 nanoparticles (ZCe1), which has sharp peaks. The pattern indicates high degree of crystallinity. These peaks can be ascribed to ZrO_2. The structure is in mixed phase of Monoclinic and Tetragonal. The observed XRD peaks are indexed as (110), ($\bar{1}$11), (101), (020), ($\bar{2}$11), (112), ($\bar{1}$22), (013), ($\bar{3}$02), (311), (320) and (400). The peak at 2θ value of 30.06º has the highest intensity, which is the most prominent peak of (101) plane of tetragonal phase matching with JCPDS card no. 79-1770. The second highest value of intensity of 614.95 is seen at 2θ value of 50.53º corresponding to ($\bar{1}$22) plane match with JCPDS card no. 83-0944 for ZrO_2 monoclinic phase. Thereafter, third highest peak intensity observed at 2θ value of 28.28º is for ($\bar{1}$11) plane of monoclinic phase as shown in **Table 4.2** [2]. Only the highest and fifth highest peak match with JCPDS card no. 79-1770 for ZrO_2 tetragonal phase. The d-values of all the other peaks match with those reported in the JCPDS card no. 83-0944 for ZrO_2 monoclinic phase.

Figures 4.2(a) to **4.7(a)** show the XRD pattern for samples ZRE1 (RE= Dy, Er, Eu, Pr, Tb, Tm). These patterns are identical to the XRD pattern of sample ZCe1. They also indicate high degree of crystallinity. The peak at 2θ value around 30º has the highest intensity in all the samples corresponding to (101) plane of tetragonal ZrO_2. Only the highest and fifth highest peak match with JCPDS card no. 79-1770 for ZrO_2 tetragonal phase. The d-values of all the other peaks match with those reported in the JCPDS card no. 83-0944 for ZrO_2 monoclinic phase as shown in **Tables 4.3** to **4.8**.

There are no other peaks detected in these XRD patterns. It confirms the formation of material in pure form with good amount of crystallinity. The peaks are broad, which might be due to the formation of material in nano scale.

The average crystallite size of the samples is calculated by Scherrer formula [1]. The average crystallite size, evident from the broadening of XRD peaks, is found to be in nanometer. The calculated values are given in **Table 4.9**.

Figures 4.1(b) to **4.7(b)** show the EDS spectra of 0.1 mol% RE doped ZrO_2 (ZRE1) sample. They indicate the presence of Zirconium, Oxygen and rare earth dopant. The results obtained from EDS are shown in **Table 4.11** in terms of Atomic%. It is observed that synthesized samples are slightly oxygen rich, which may be due to calcination of the samples.

The average diameter for 0.1 mol% RE doped ZrO_2 (ZRE1) samples dispersed in water were also measured using particle size analyzer by Dynamic Light Scattering (DLS) technique. **Figures 4.1(c)** to **4.7(c)** show the DLS results of the samples. The majority of the particles are distributed in the range of 54-69 nm. There is a short tail towards the larger particle size showing the residual particles. These larger particles could not be eliminated even after extended sonication. The distribution of diameter of the particles is shown in **Table 4.10**.

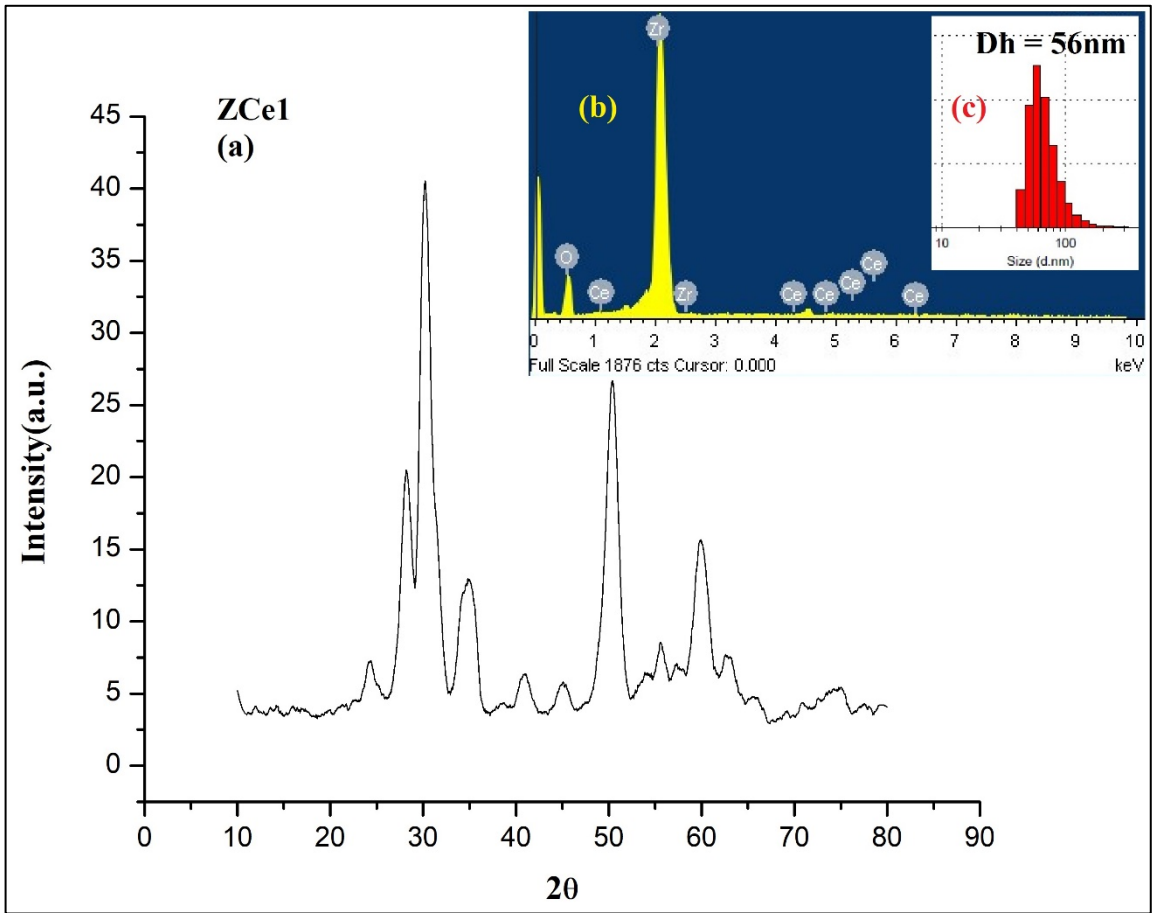

Figure 4.1: XRD pattern (a), EDS spectra (b) and DLS pattern (c) of ZCe1

Table 4.2: Structural parameters of Ce doped ZrO_2 sample (ZCe1)

2θ ZCe1	Intensity I/I0	Calculated d values	JCPDS d values 83-0944 M 79-1770 T	hkl
24.69	133.84	3.6475	3.6323	(110)
28.28	512.84	3.1556	3.1598	$(\bar{1}11)$
30.06	1000	2.9727	2.9529	(101)
34.57	260.68	2.5946	2.5907	(002)
40.89	97.37	2.2069	2.2110	$(\bar{2}11)$
45.01	99.06	2.0141	2.0187	(112)
50.53	614.95	1.8062	1.8012	$(\bar{1}22)$
55.59	180.04	1.6533	1.6565	(013)
60.41	308.02	1.5323	1.5381	$(\bar{3}02)$
63.09	158.04	1.4737	1.4764	(311)
65.60	106.66	1.4231	1.4187	(320)
74.77	81.83	1.2698	1.2690	(400)

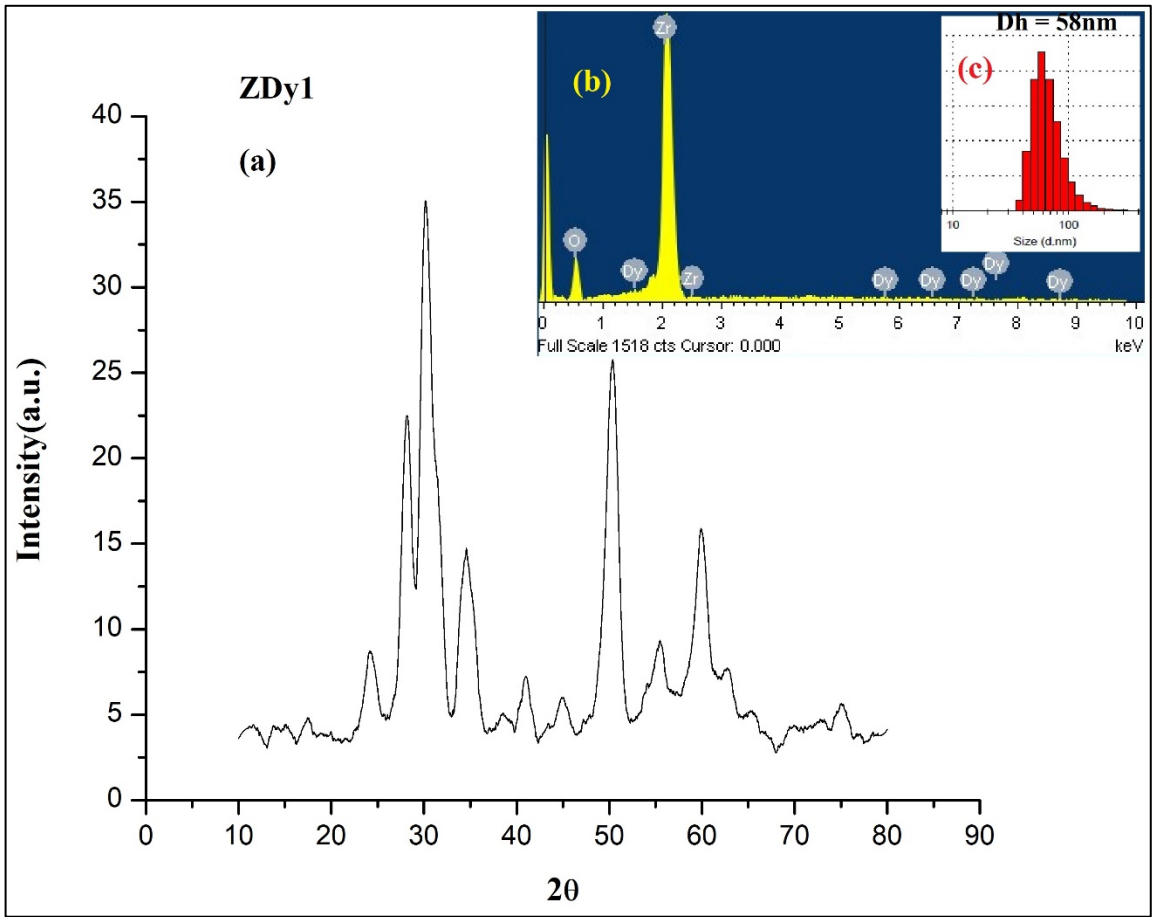

Figure 4.2: XRD pattern (a), EDS spectra (b) and DLS pattern (c) of ZDy1

Table 4.3: Structural parameters of Dy doped ZrO_2 sample (ZDy1)

2θ ZDy1	Intensity I/I0	Calculated d values	JCPDS d values 83-0944 M 79-1770 T	hkl
24.60	180.76	3.6182	3.6323	(110)
28.06	664.21	3.1803	3.1598	$(\bar{1}11)$
30.06	1000	2.9729	2.9529	(101)
35.04	349.46	2.5610	2.5411	(110)
40.70	158.83	2.2170	2.2110	$(\bar{2}11)$
44.86	98.64	2.0207	2.0187	(112)
50.28	747.69	1.8146	1.8161	(220)
55.39	188.19	1.6586	1.6565	(013)
60.20	267.69	1.5372	1.5381	$(\bar{3}02)$
62.50	160.11	1.4861	1.4764	(311)
65.82	91.71	1.4189	1.4187	(320)
74.78	99.84	1.2695	1.2690	(400)

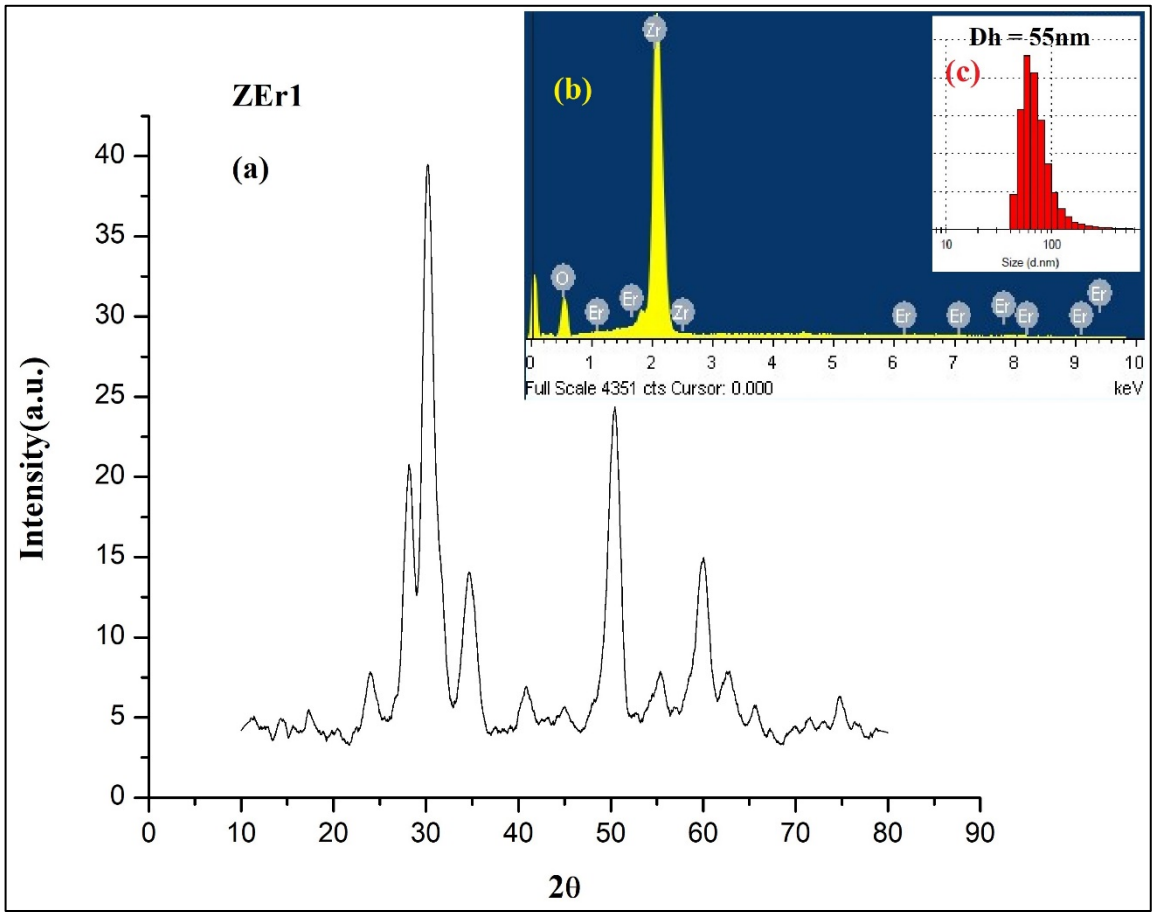

Figure 4.3: XRD pattern (a), EDS spectra (b) and DLS pattern (c) of ZEr1

Table 4.4: Structural parameters of Er doped ZrO_2 sample (ZEr1)

2θ ZEr1	Intensity I/I0	Calculated d values	JCPDS d values 83-0944 M 79-1770 T	hkl
24.07	169.55	3.6972	3.6919	(011)
28.19	459.18	3.1656	3.1598	$(\bar{1}11)$
30.19	1000	2.9605	2.9529	(101)
34.70	255.87	2.5850	2.5907	(002)
41.04	138.58	2.1995	2.1906	(102)
44.77	105.68	2.0243	2.0187	(112)
50.41	568.02	1.8103	1.8161	(220)
55.26	132.63	1.6623	1.6565	(013)
60.00	369.21	1.5419	1.5381	$(\bar{3}02)$
62.68	170.24	1.4822	1.4764	(311)
65.88	102.54	1.4177	1.4187	(320)
75.23	95.04	1.2630	1.2690	(400)

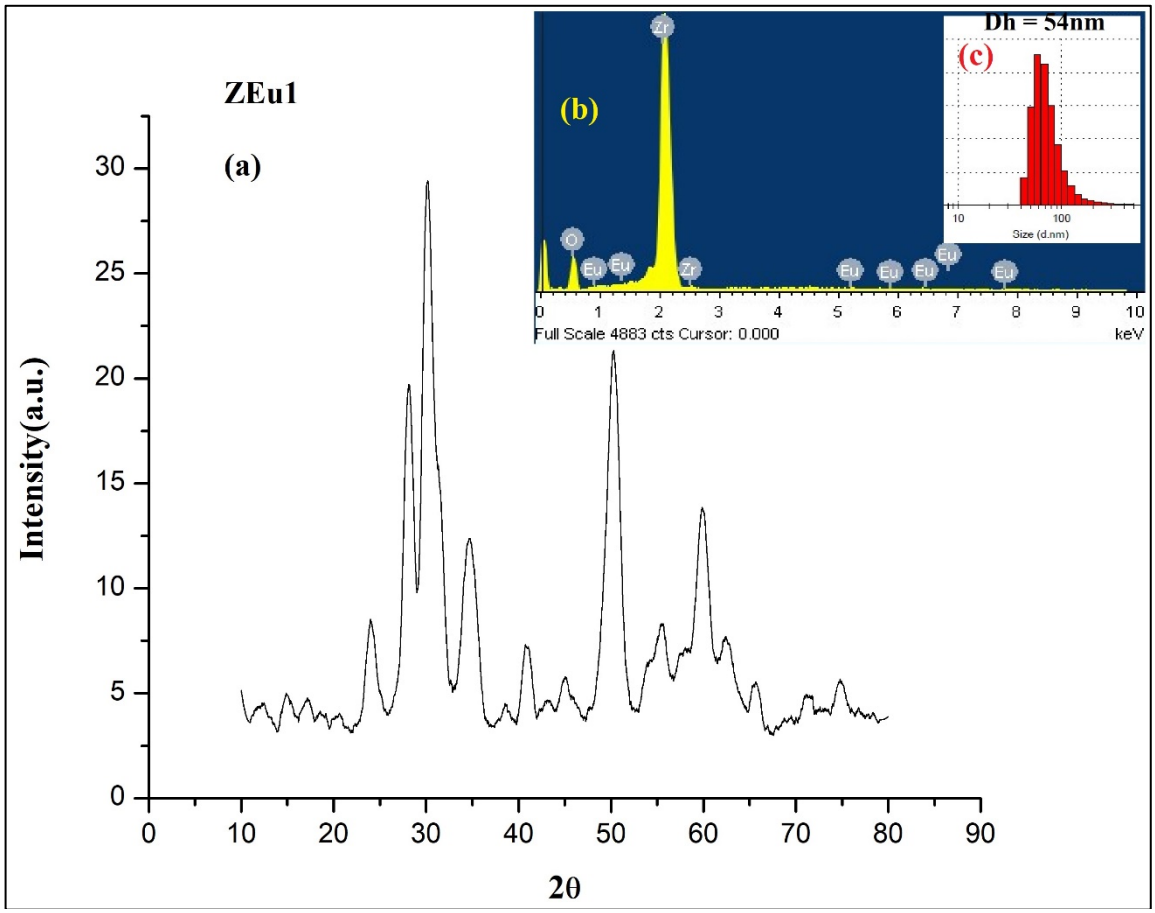

Figure 4.4: XRD pattern (a), EDS spectra (b) and DLS pattern (c) of ZEu1

Table 4.5: Structural parameters of Eu doped ZrO_2 sample (ZEu1)

2θ ZEu1	Intensity I/I0	Calculated d values	JCPDS d values 83-0944 M 79-1770 T	hkl
24.04	221.16	3.7018	3.6919	(011)
28.08	622.77	3.1648	3.1598	$(\bar{1}11)$
30.16	1000	2.9631	2.9529	(101)
34.72	322.15	2.5919	2.5907	(002)
41.07	210.27	2.1979	2.1906	(102)
44.76	148.40	2.0248	2.0187	(112)
50.38	669.27	1.8112	1.8161	(220)
54.90	190.83	1.6724	1.6752	(122)
60.08	347.54	1.5401	1.5381	$(\bar{3}02)$
62.70	180.08	1.4817	1.4764	(311)
65.76	108.86	1.4201	1.4187	(320)
75.00	122.91	1.2664	1.2690	(400)

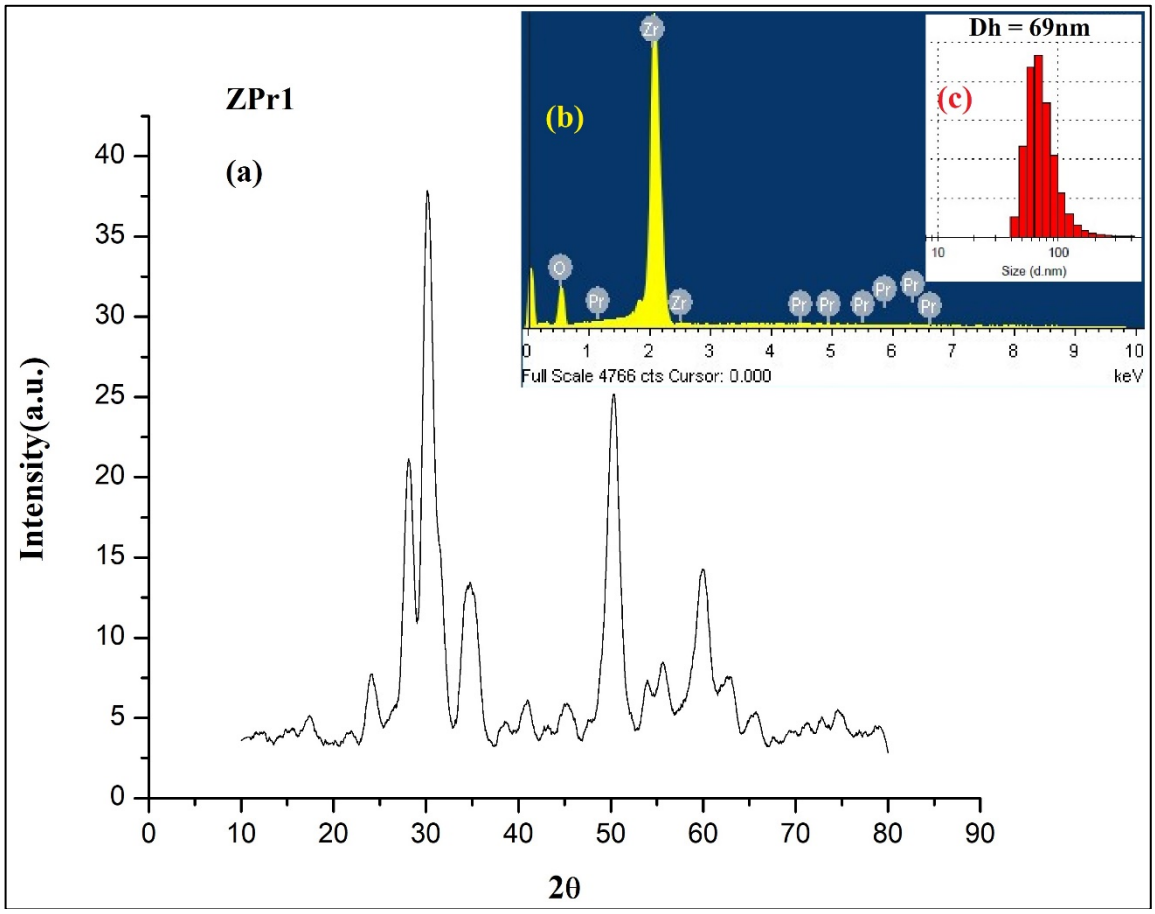

Figure 4.5: XRD pattern (a), EDS spectra (b) and DLS pattern (c) of ZPr1

Table 4.6: Structural parameters of Pr doped ZrO_2 sample (ZPr1)

2θ ZPr1	Intensity I/I0	Calculated d values	JCPDS d values 83-0944 M 79-1770 T	hkl
24.52	133.20	3.6303	3.6323	(110)
28.09	536.43	3.1766	3.1598	$(\bar{1}11)$
30.23	1000	2.9632	2.9529	(101)
35.49	298.82	2.5294	2.5411	(110)
40.89	120.06	2.2069	2.2110	$(\bar{2}11)$
45.06	144.61	2.0122	2.0187	(112)
50.20	652.91	1.8175	1.8161	(220)
55.98	163.39	1.6427	1.6457	(031)
59.94	312.34	1.5433	1.5429	(131)
62.28	122.24	1.4909	1.4948	$(\bar{2}13)$
65.81	71.27	1.4192	1.4187	(320)
74.94	70.34	1.2672	1.2690	(400)

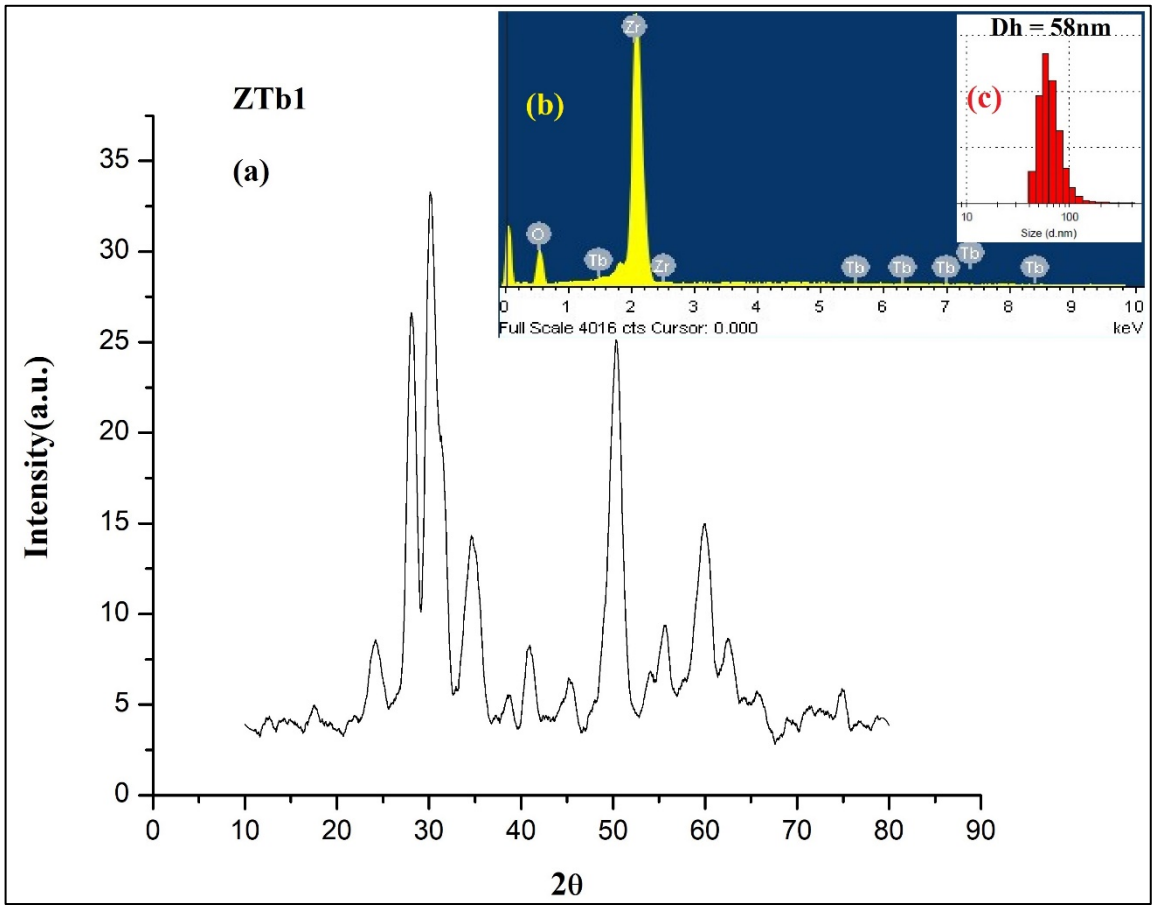

Figure 4.6: XRD pattern (a), EDS spectra (b) and DLS pattern (c) of ZTb1

Table 4.7: Structural parameters of Tb doped ZrO_2 sample (ZTb1)

2θ ZTb1	Intensity I/I0	Calculated d values	JCPDS d values 83-0944 M 79-1770 T	hkl
24.13	186.58	3.6879	3.6919	(011)
28.23	776.07	3.1613	3.1598	$(\bar{1}11)$
30.32	1000	2.9475	2.9529	(101)
34.48	329.48	2.6014	2.5907	(002)
41.32	169.44	2.1851	2.1906	(102)
44.10	139.20	2.0535	2.0622	(121)
50.25	643.79	1.8156	1.8161	(220)
55.34	218.43	1.6601	1.6565	(013)
60.13	407.42	1.5388	1.5381	$(\bar{3}02)$
62.79	196.61	1.4800	1.4764	(311)
65.87	127.70	1.4179	1.4187	(320)
74.78	124.71	1.2696	1.2690	(400)

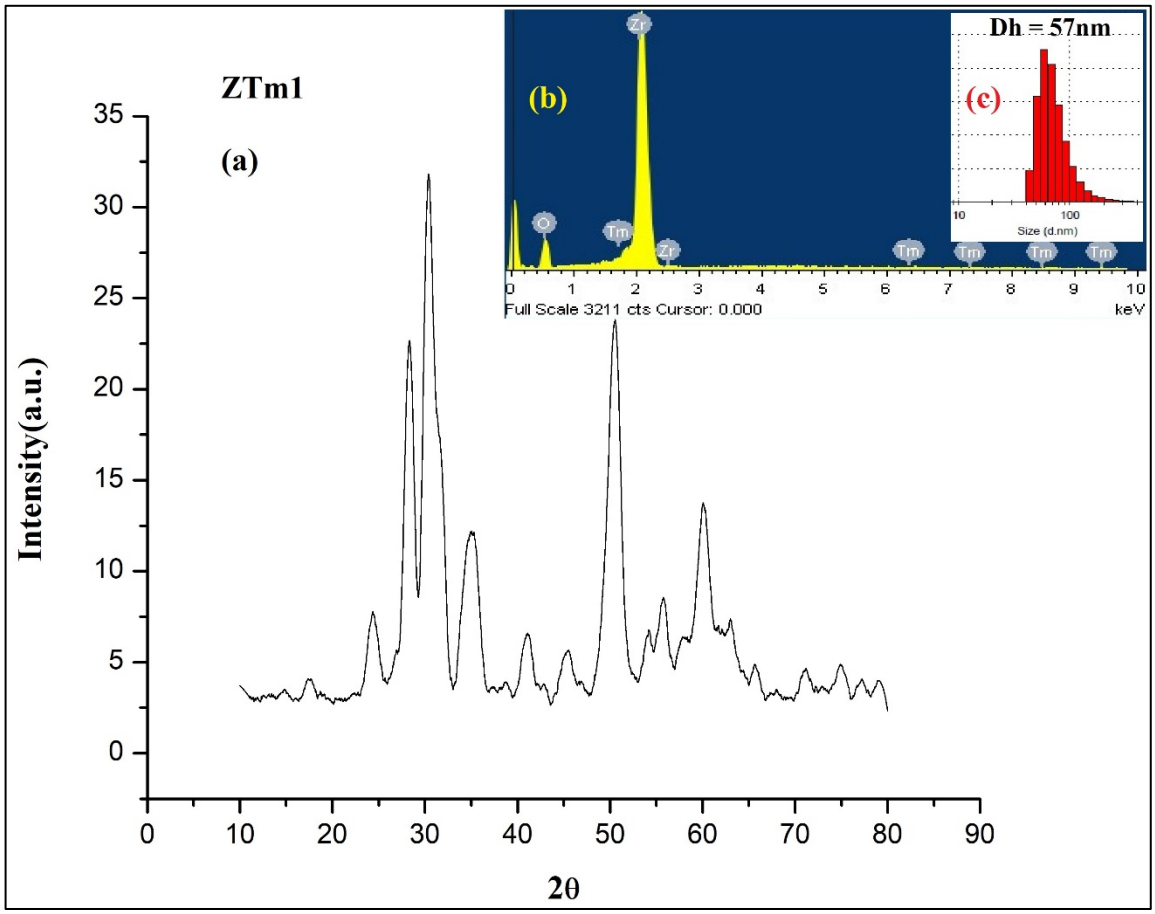

Figure 4.7: XRD pattern (a), EDS spectra (b) and DLS pattern (c) of ZTm1

Table 4.8: Structural parameters of Tm doped ZrO_2 sample (ZTm1)

2θ ZTm1	Intensity I/I0	Calculated d values	JCPDS d values 83-0944 M 79-1770 T	hkl
24.29	213.93	3.6939	3.6919	(011)
28.38	633.17	3.1447	3.1598	$(\bar{1}11)$
30.35	1000	2.9454	2.9529	(101)
34.89	314.02	2.5809	2.5907	(002)
40.63	121.86	2.2206	2.2110	$(\bar{2}11)$
45.43	137.92	1.9965	1.9893	(211)
50.40	659.34	1.8107	1.8161	(220)
55.55	239.71	1.6544	1.6565	(013)
60.38	372.68	1.5330	1.5381	$(\bar{3}02)$
61.93	180.98	1.4985	1.4948	$(\bar{2}13)$
65.87	148.55	1.4179	1.4187	(320)
75.23	140.28	1.2632	1.2690	(400)

The average crystallite sizes, thus calculated and given in **Table 4.9**. The results clearly indicate that the samples are in nanocrystalline phase, and the crystallite size varies from 5.18 nm to 8.11 nm.

Table 4.9: Crystallite size for ZRE1 (RE= Ce, Dy, Er, Eu, Pr, Tb, Tm) samples

Sample	Crystallite Size (nm)
ZCe1	**7.87**
ZDy1	**6.24**
ZEr1	**8.11**
ZEu1	**6.42**
ZPr1	**5.78**
ZTb1	**7.20**
ZTm1	**5.18**

Table 4.10: Distribution of Diameter of ZRE1 samples

Sample	Diameter D_h (nm)
ZCe1	**56**
ZDy1	**58**
ZEr1	**55**
ZEu1	**54**
ZPr1	**69**
ZTb1	**58**
ZTm1	**57**

Table 4.11: Elemental composition of ZRE1 samples obtained from EDS

Sample	Atomic %	
	Zr	**O**
ZCe1	24.89	74.97
ZDy1	25.26	74.54
ZEr1	26.33	73.53
ZEu1	26.74	73.14
ZPr1	25.78	74.09
ZTb1	26.26	73.58
ZTm1	26.92	72.87

The XRD patterns of 0.2 mol% RE doped ZrO_2 nanoparticles (ZRE2) are shown in **Figures 4.8(a)** to **4.14(a).** The structural parameters are given in **Table 4.12** to **4.18**.

Figures 4.8(a) to **4.14(a)** represent the XRD pattern for ZRE2 (RE= Ce, Dy, Er, Eu, Pr, Tb, Tm) samples. They are quite identical with each other and to the XRD pattern of TRE1 samples as well. The structure is in mixed phase of Monoclinic and Tetragonal. The peak at 2θ value around 30º has the highest intensity in all the samples corresponding to (101) plane of tetragonal ZrO_2. Only the highest and fifth highest peak match with JCPDS card no. 79-1770 for ZrO_2 tetragonal phase. The d-values of all the other peaks match with those reported in the JCPDS card no. 83-0944 for ZrO_2 monoclinic phase as shown in **Tables 4.12** to **4.18**.

The average crystallite size for ZrO_2:RE samples with 0.2 mol% doping concentration of rare earth elements (ZRE2) are given in **Table 4.19**.

Figures 4.8(b) to **4.14(b)** show the EDS spectra of 0.2 mol% RE doped ZrO_2 (ZRE2) sample which indicates the presence of Zirconium, Oxygen and rare earth elements thus showing the purity of the sample. The results of EDS are shown in **Table 4.21** in terms of Atomic%. It is observed that synthesized samples are slightly oxygen rich which may be due to calcination of the samples.

The average diameter (D_h) for 0.2 mol% RE doped ZrO_2 (ZRE2) samples dispersed in water were also measured using particle size analyzer by Dynamic Light Scattering (DLS) technique. **Figures 4.8(c)** to **4.14(c)** show the DLS results of ZRE2 samples indicating the range of distribution is 55 nm to 64 nm with a short tail towards the larger particle size shown in particle size histogram. The larger particles could not be eliminated even after extended sonication. The distribution of diameter of the particles are found in nanometer range as shown in **Table 4.20**.

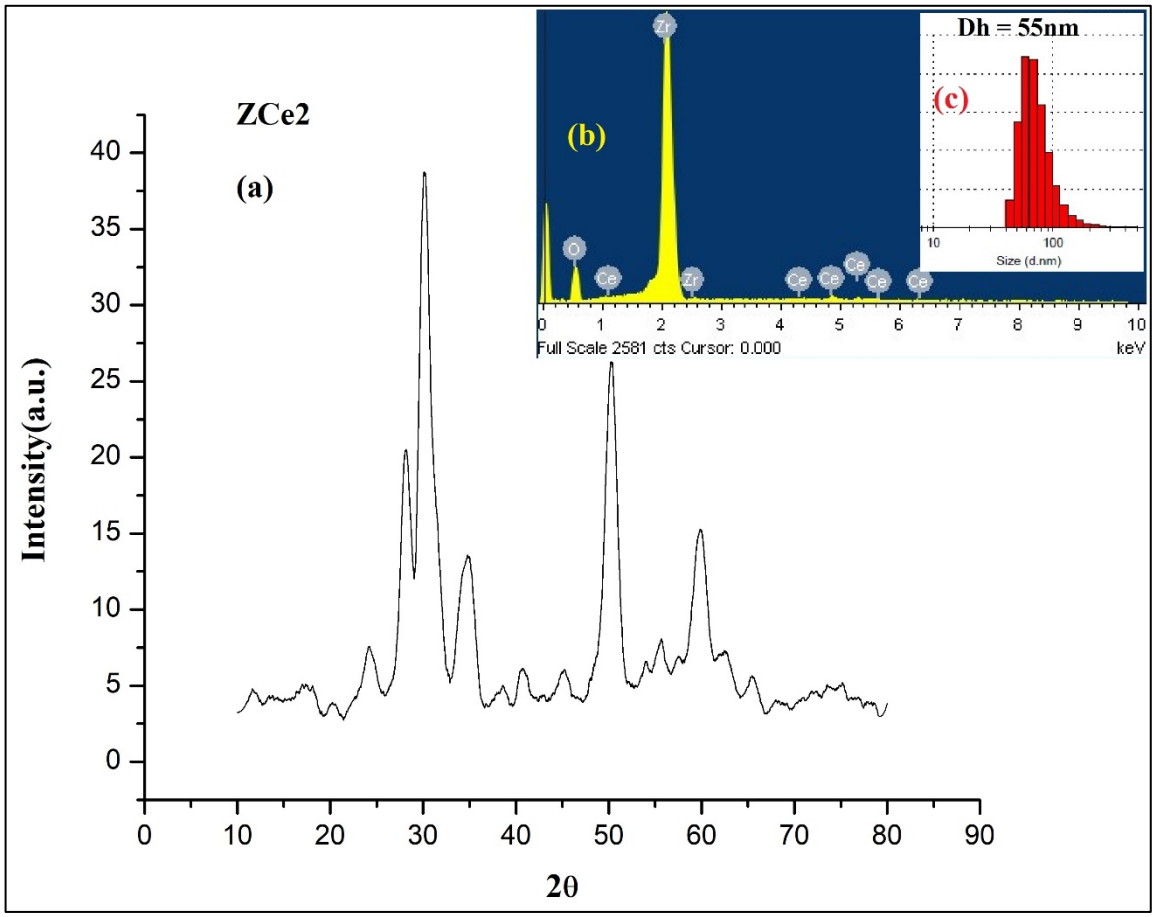

Figure 4.8: XRD pattern (a), EDS spectra (b) and DLS pattern (c) of ZCe2

Table 4.12: Structural parameters of Ce doped ZrO_2 sample (ZCe2)

2θ ZCe2	Intensity I/I0	Calculated d values	JCPDS d values 83-0944 M 79-1770 T	hkl
24.28	156.19	3.6952	3.6919	(011)
28.40	475.82	3.1602	3.1598	$(\bar{1}11)$
30.11	1000	2.9685	2.9529	(101)
34.78	269.94	2.5998	2.5907	(002)
40.51	104.06	2.2268	2.2110	$(\bar{2}11)$
45.28	81.92	2.0028	2.0187	(112)
50.15	610.00	1.8190	1.8161	(220)
55.55	144.84	1.6545	1.6565	(013)
60.00	349.84	1.5420	1.5381	$(\bar{3}02)$
61.76	107.93	1.5021	1.5087	(113)
65.34	73.67	1.4281	1.4240	$(\bar{1}32)$
73.82	90.30	1.2837	1.2850	$(\bar{3}13)$

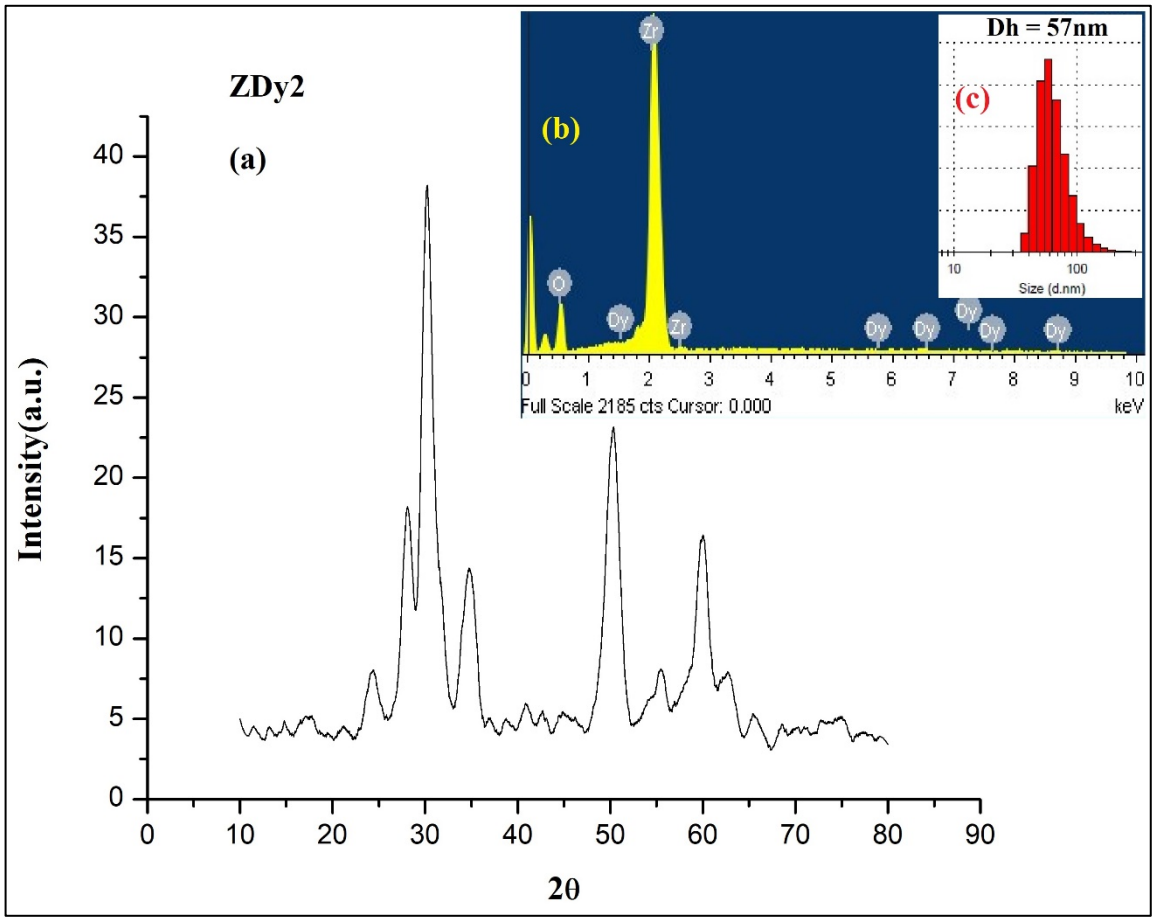

Figure 4.9: XRD pattern (a), EDS spectra (b) and DLS pattern (c) of ZDy2

Table 4.13: Structural parameters of Dy doped ZrO_2 sample (ZDy2)

2θ ZDy2	Intensity I/I0	Calculated d values	JCPDS d values 83-0944 M 79-1770 T	hkl
24.29	136.78	3.7050	3.6919	(011)
28.03	417.35	3.1667	3.1598	$(\bar{1}11)$
30.33	1000	2.9474	2.9529	(101)
35.01	345.81	2.5462	2.5411	(110)
40.87	105.27	2.2083	2.2110	$(\bar{2}11)$
43.78	110.44	2.0676	2.0622	(121)
50.28	558.08	1.8149	1.8161	(220)
55.73	166.50	1.6496	1.6503	$(\bar{1}13)$
59.91	410.63	1.5441	1.5429	(131)
62.52	162.63	1.4857	1.4764	(311)
65.31	94.98	1.4287	1.4240	$(\bar{1}32)$
75.37	111.00	1.2611	1.2617	(041)

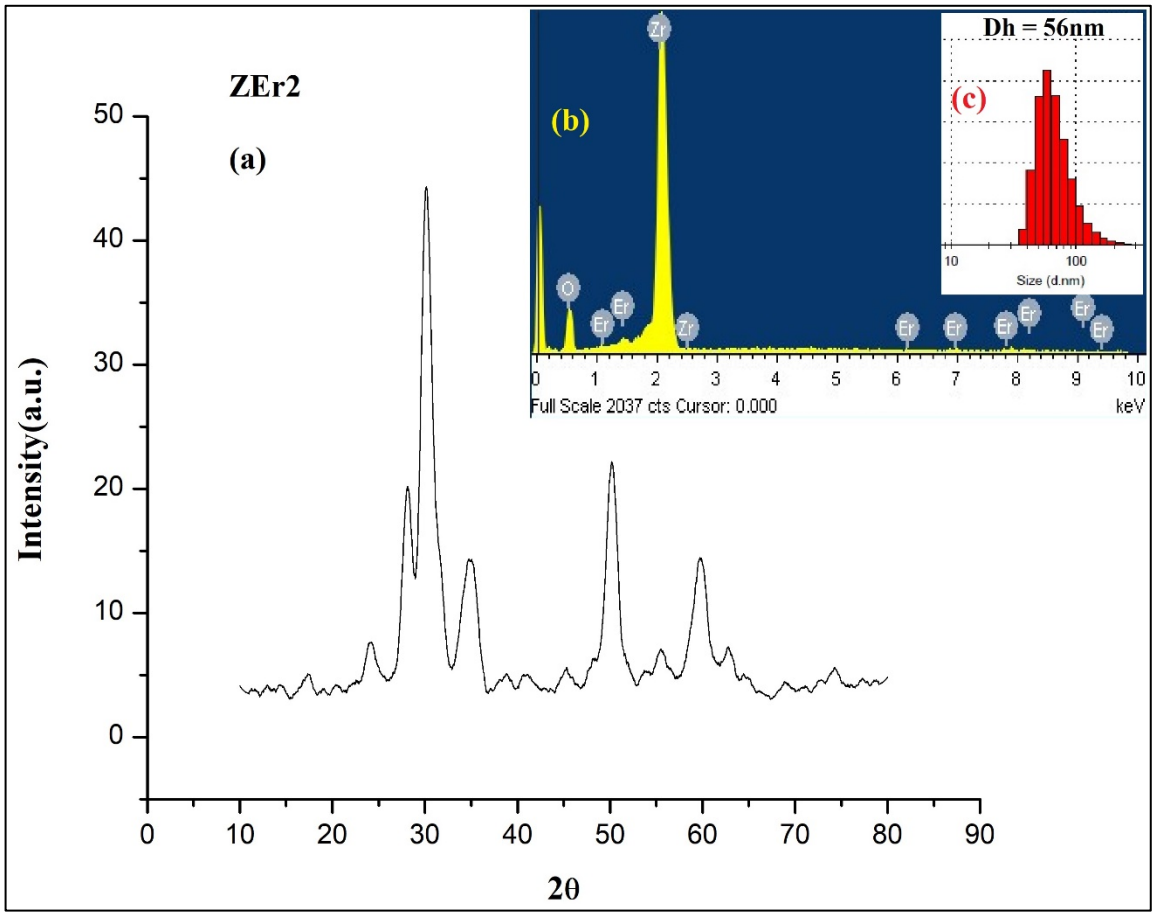

Figure 4.10: XRD pattern (a), EDS spectra (b) and DLS pattern (c) of ZEr2

Table 4.14: Structural parameters of Er doped ZrO_2 sample (ZEr2)

2θ ZEr2	Intensity I/I0	Calculated d values	JCPDS d values 83-0944 M 79-1770 T	hkl
24.36	174.20	3.6536	3.6323	(110)
28.26	458.99	3.1578	3.1598	$(\bar{1}11)$
30.24	1000	2.9557	2.9529	(101)
35.04	282.56	2.5367	2.5411	(110)
40.72	111.62	2.2161	2.2110	$(\bar{2}11)$
43.98	70.65	2.0589	2.0622	(121)
50.27	614.98	1.8152	1.8161	(220)
55.51	152.88	1.6554	1.6565	(013)
60.33	405.38	1.5343	1.5381	$(\bar{3}02)$
62.76	170.29	1.4804	1.4764	(311)
65.73	93.11	1.4206	1.4187	(320)
75.00	113.95	1.2665	1.2690	(400)

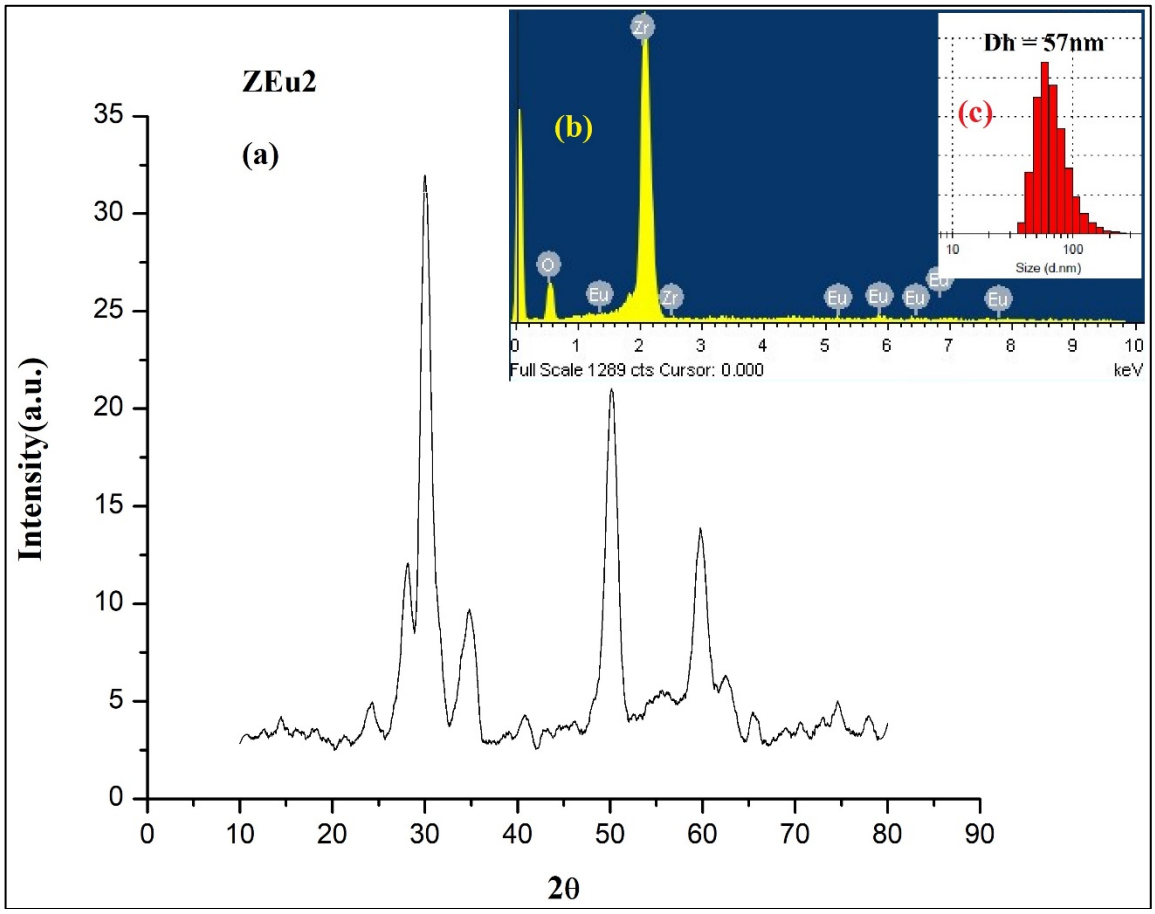

Figure 4.11: XRD pattern (a), EDS spectra (b) and DLS pattern (c) of ZEu2

Table 4.15: Structural parameters of Eu doped ZrO_2 sample (ZEu2)

2θ ZEu2	Intensity I/I0	Calculated d values	JCPDS d values 83-0944 M 79-1770 T	hkl
24.24	128.12	3.6762	3.6919	(011)
28.17	363.36	3.1677	3.1598	$(\bar{1}11)$
30.05	1000	2.9738	2.9529	(101)
34.89	253.55	2.5718	2.5907	(002)
40.86	102.48	2.2087	2.2110	$(\bar{2}11)$
46.44	107.72	1.9552	1.9893	(211)
50.29	643.43	1.8145	1.8161	(220)
54.38	152.35	1.6872	1.6752	(122)
59.94	412.45	1.5434	1.5429	(131)
62.62	187.80	1.4835	1.4764	(311)
65.59	156.08	1.4234	1.4187	(320)
74.60	132.29	1.2722	1.2690	(400)

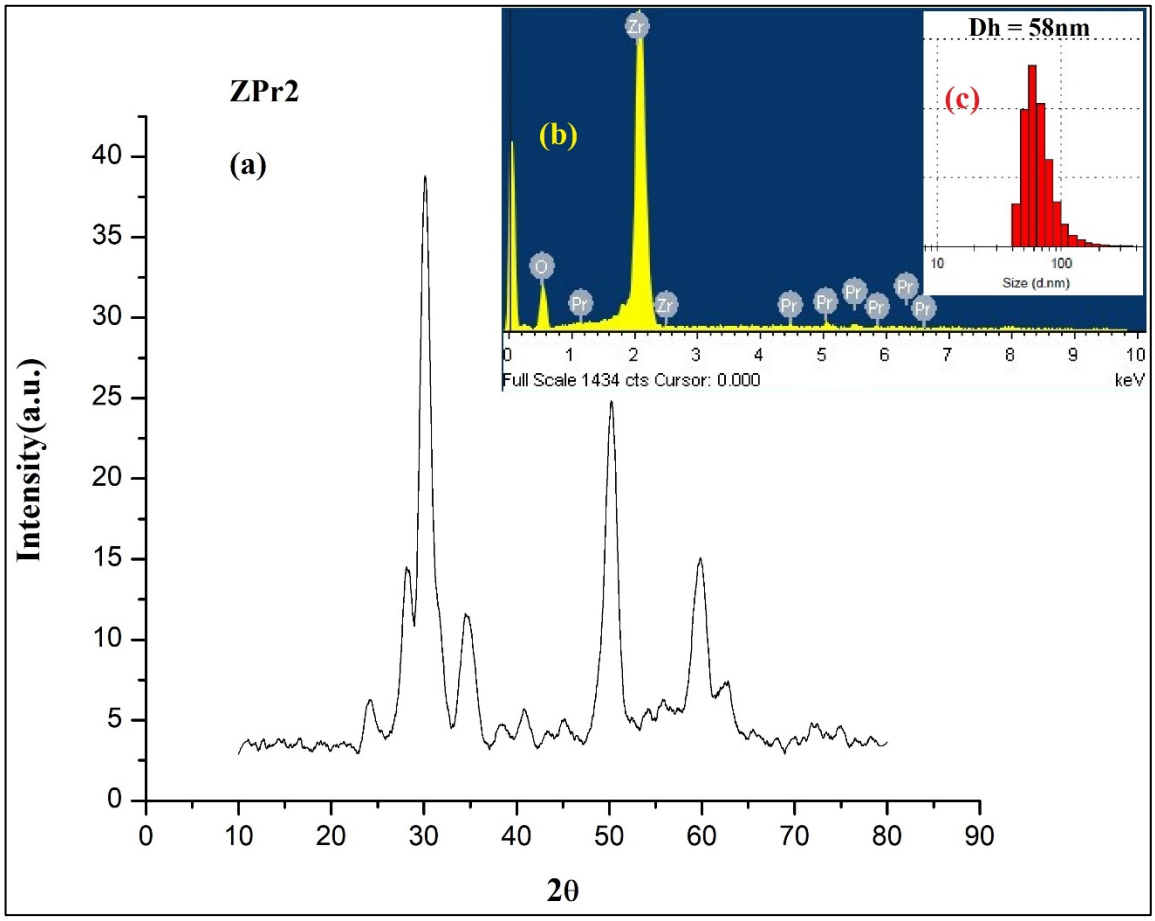

Figure 4.12: XRD pattern (a), EDS spectra (b) and DLS pattern (c) of ZPr2

Table 4.16: Structural parameters of Pr doped ZrO_2 sample (ZPr2)

2θ ZPr2	Intensity I/I0	Calculated d values	JCPDS d values 83-0944 M 79-1770 T	hkl
23.87	143.01	3.7180	3.6919	(011)
28.12	383.72	3.1733	3.1598	$(\bar{1}11)$
30.10	1000	2.9691	2.9529	(101)
34.84	249.14	2.5749	2.5907	(002)
40.54	129.60	2.2253	2.2110	$(\bar{2}11)$
45.32	127.92	2.0010	2.0187	(112)
50.20	599.76	1.8174	1.8161	(220)
55.50	174.87	1.6558	1.6565	(013)
59.64	350.55	1.5503	1.5429	(131)
62.64	165.86	1.4831	1.4764	(311)
65.94	119.46	1.4166	1.4187	(320)
74.95	113.85	1.2671	1.2690	(400)

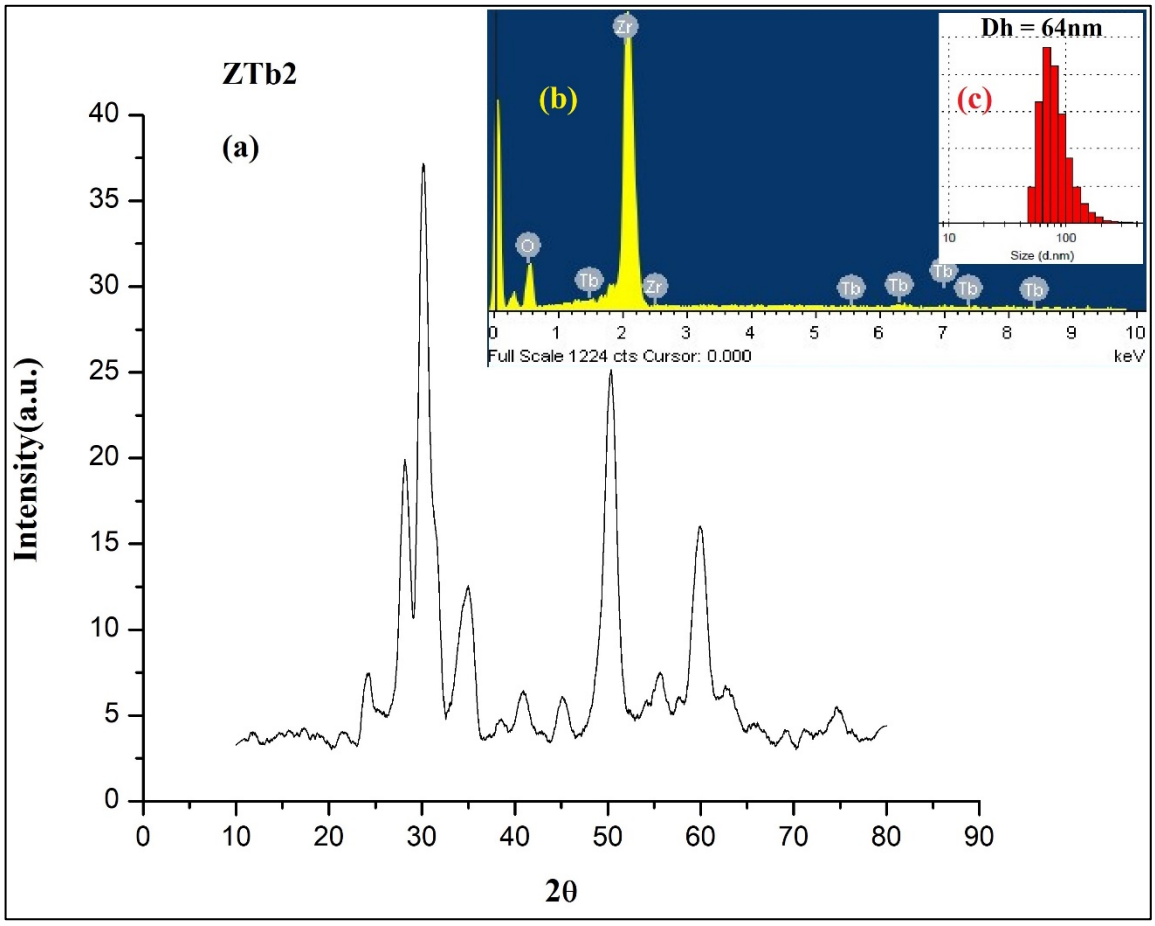

Figure 4.13: XRD pattern (a), EDS spectra (b) and DLS pattern (c) of ZTb2

Table 4.17: Structural parameters of Tb doped ZrO_2 sample (ZTb2)

2θ ZTb2	Intensity I/I0	Calculated d values	JCPDS d values 83-0944 M 79-1770 T	hkl
24.00	163.25	3.7085	3.6919	(011)
28.26	544.45	3.1580	3.1598	$(\bar{1}11)$
30.13	1000	2.9662	2.9529	(101)
35.37	282.15	2.5380	2.5411	(110)
41.04	152.35	2.1993	2.1906	(102)
44.35	110.15	2.0425	2.0187	(112)
50.25	643.38	1.8157	1.8161	(220)
55.52	191.24	1.6553	1.6565	(013)
60.08	390.01	1.5399	1.5381	$(\bar{3}02)$
62.80	175.99	1.4798	1.4764	(311)
65.71	122.69	1.4211	1.4187	(320)
75.26	105.45	1.2627	1.2690	(400)

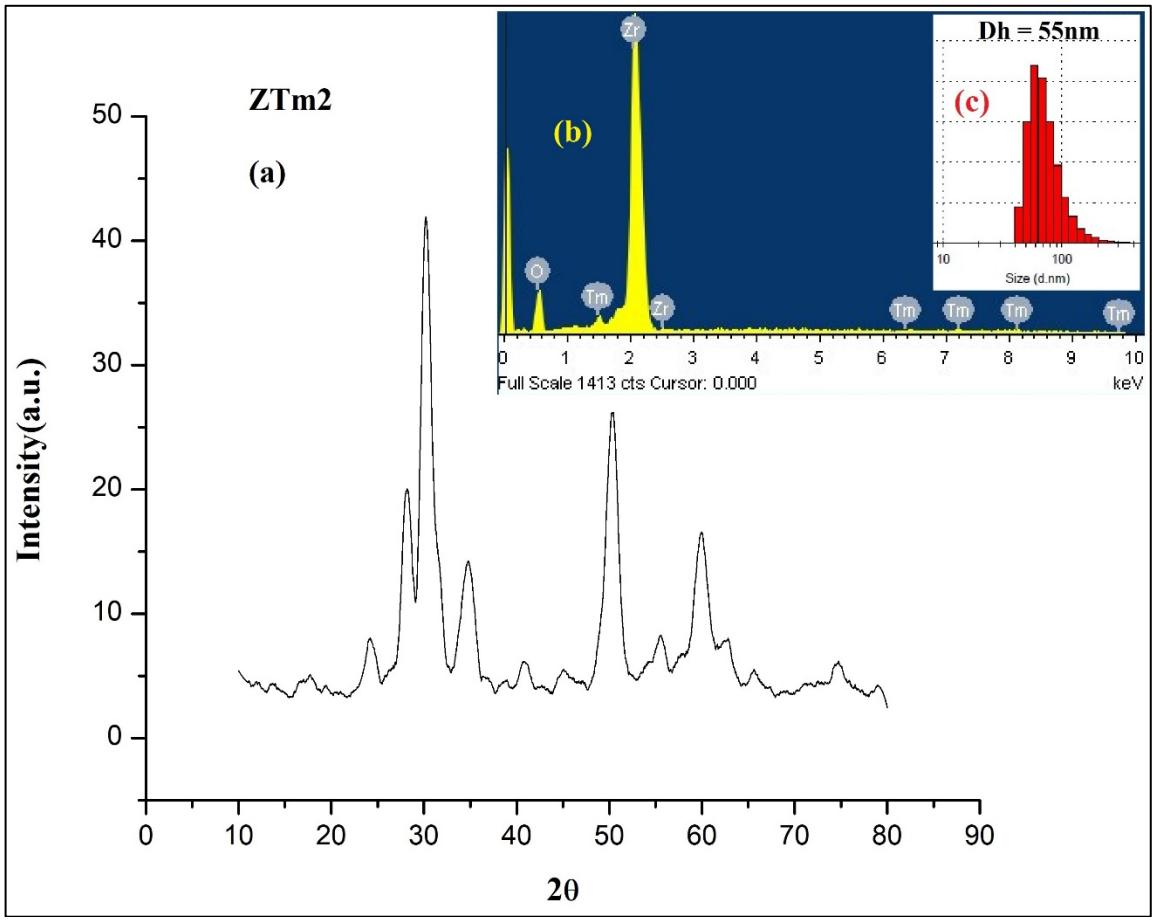

Figure 4.14: XRD pattern (a), EDS spectra (b) and DLS pattern (c) of ZTm2

Table 4.18: Structural parameters of Tm doped ZrO_2 sample (ZTm2)

2θ ZTm2	Intensity I/I0	Calculated d values	JCPDS d values 83-0944 M 79-1770 T	hkl
24.54	151.10	3.6280	3.6323	(110)
28.23	463.29	3.1617	3.1598	$(\bar{1}11)$
30.35	1000	2.9455	2.9529	(101)
35.28	273.98	2.5443	2.5411	(110)
41.02	129.18	2.2003	2.1906	(102)
44.77	152.97	2.0244	2.0187	(112)
50.31	583.44	1.8137	1.8161	(220)
55.59	172.56	1.6534	1.6565	(013)
59.67	310.29	1.5497	1.5429	(131)
62.65	180.44	1.4829	1.4764	(311)
65.62	114.39	1.4227	1.4187	(320)
74.76	132.99	1.2699	1.2690	(400)

Table 4.19: Crystallite size for ZRE2 (RE= Ce, Dy, Er, Eu, Pr, Tb, Tm) samples

Sample	Crystallite Size (nm)
ZCe2	7.35
ZDy2	5.74
ZEr2	7.92
ZEu2	6.28
ZPr2	5.69
ZTb2	6.86
ZTm2	5.57

Table 4.20: Distribution of Diameter of ZRE2 samples

Sample	Diameter D_h (nm)
ZCe2	55
ZDy2	57
ZEr2	56
ZEu2	57
ZPr2	58
ZTb2	64
ZTm2	55

Table 4.21: Elemental composition of ZRE2 samples obtained from EDS

Sample	Atomic %	
	Zr	**O**
ZCe2	26.49	72.90
ZDy2	24.23	75.34
ZEr2	26.18	73.27
ZEu2	25.96	73.71
ZPr2	25.90	73.40
ZTb2	23.61	76.00
ZTm2	25.89	73.52

Study of Composites

Samples

1. **1 mol% of RE doped ZrO_2 blended with PAA(Poly Acrylic Acid)**
2. **2 mol% of RE doped ZrO_2 blended with PAA(Poly Acrylic Acid)**

4.3.2 Fourier Transformation Infra-Red Spectroscopy (FTIR)

FTIR spectroscopic studies were done using JASCO FT/IR-4700 spectrometer recorded in the range 500-4000 cm^{-1}. FTIR spectra of pure PAA and 1 mol% ZrO_2:RE – PAA nanocomposites (PZRE1) are shown in **Figures 4.15** to **4.22**. FTIR spectra of 2 mol% ZrO_2:RE – PAA nanocomposites (PZRE2) are shown in **Figures 4.23** to **4.29**. The presence of different functional groups with respective wavenumber is shown in **Table 4.22**.

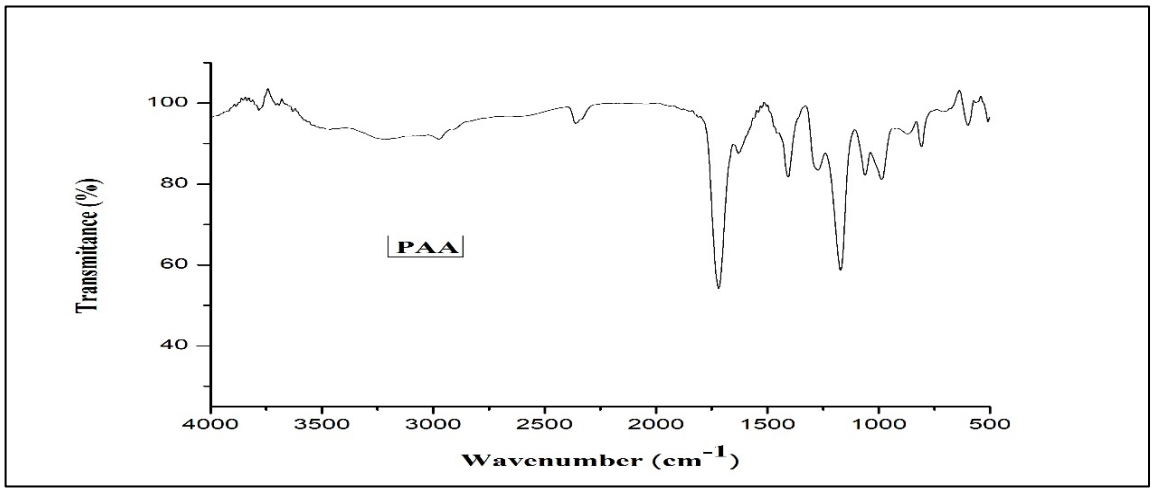

Figure 4.15: FTIR spectra of pure PAA

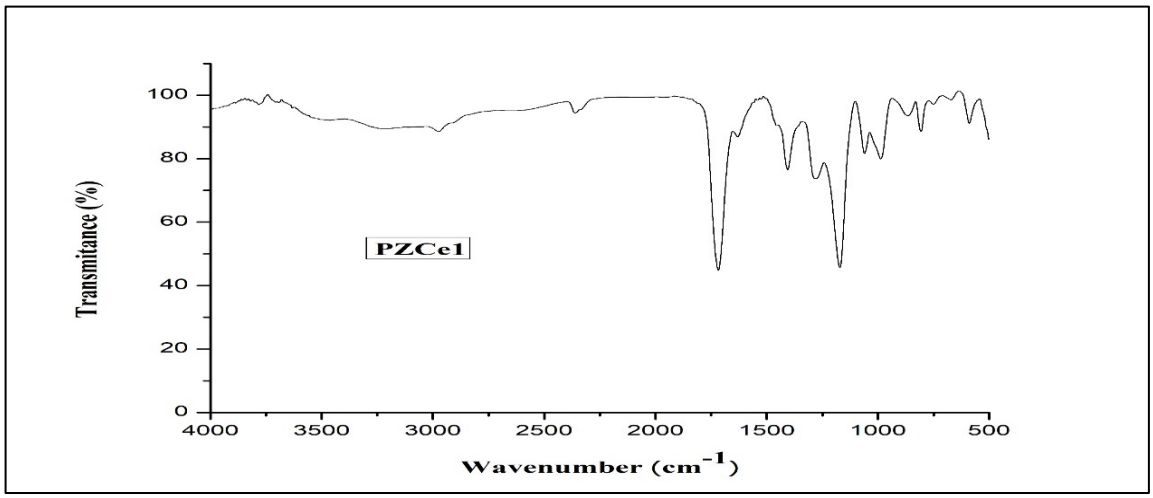

Figure 4.16: FTIR spectra of PZCe1 sample

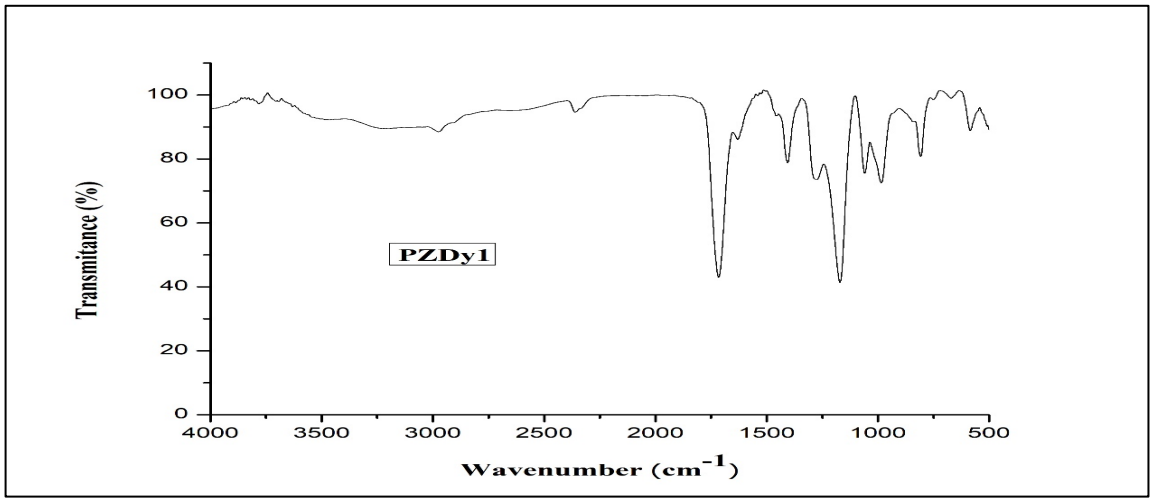

Figure 4.17: FTIR spectra of PZDy1 sample

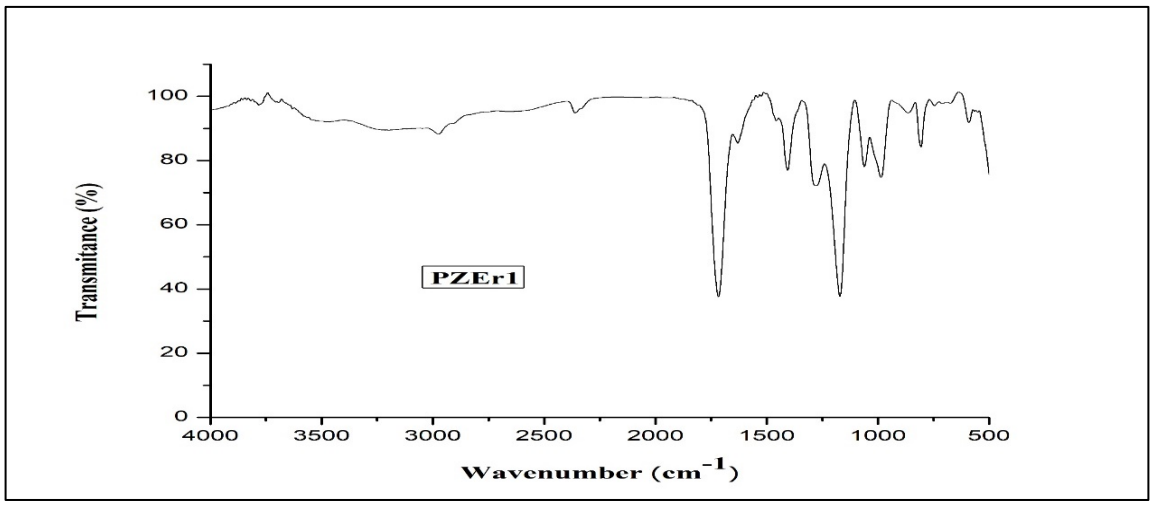

Figure 4.18: FTIR spectra of PZEr1 sample

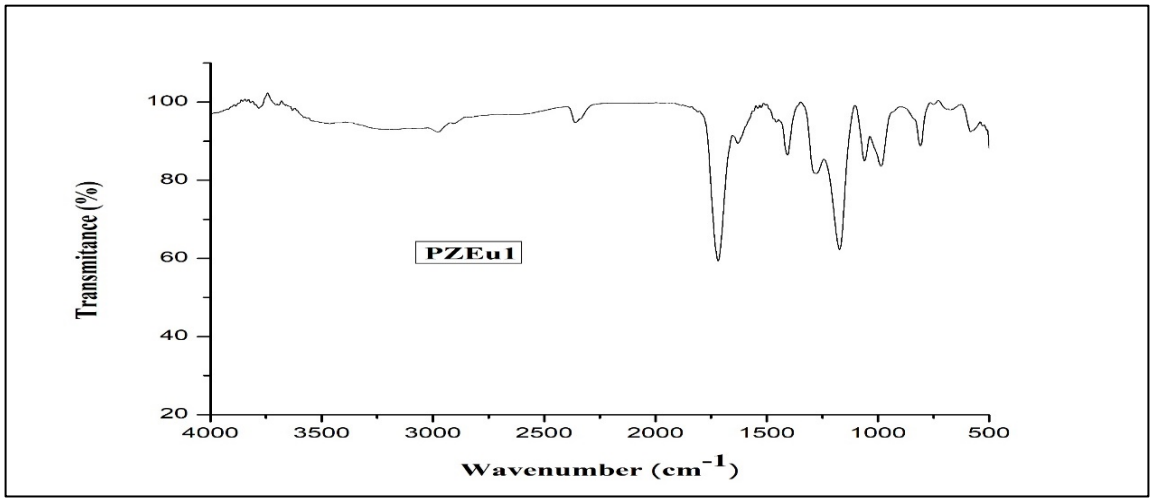

Figure 4.19: FTIR spectra of PZEu1 sample

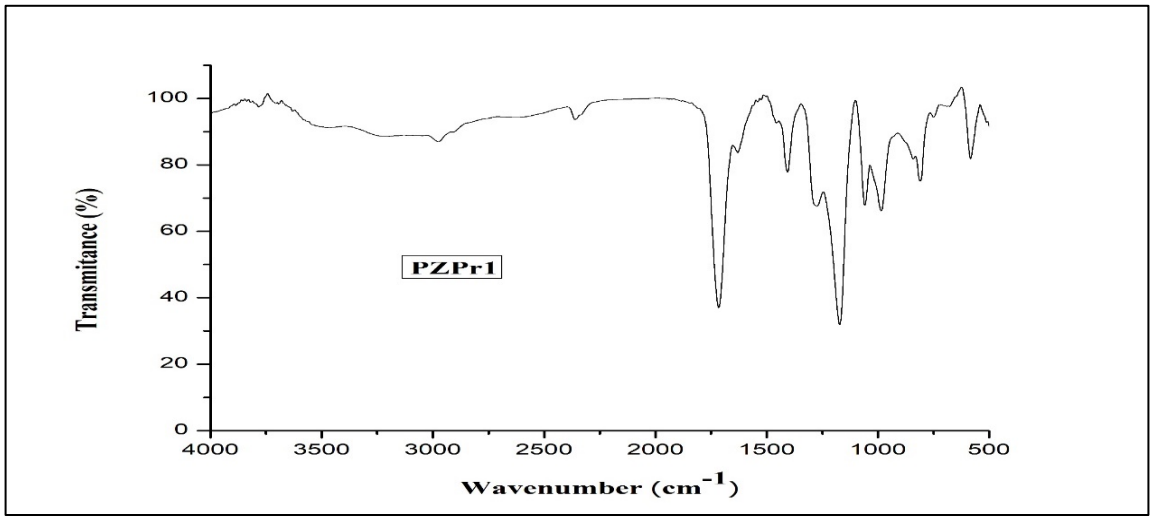

Figure 4.20: FTIR spectra of PZPr1 sample

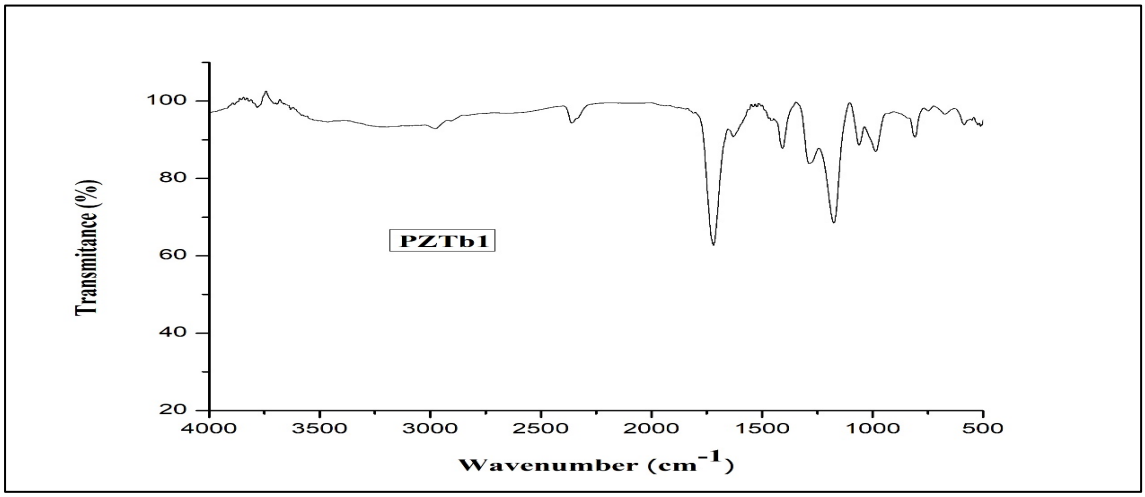

Figure 4.21: FTIR spectra of PZTb1 sample

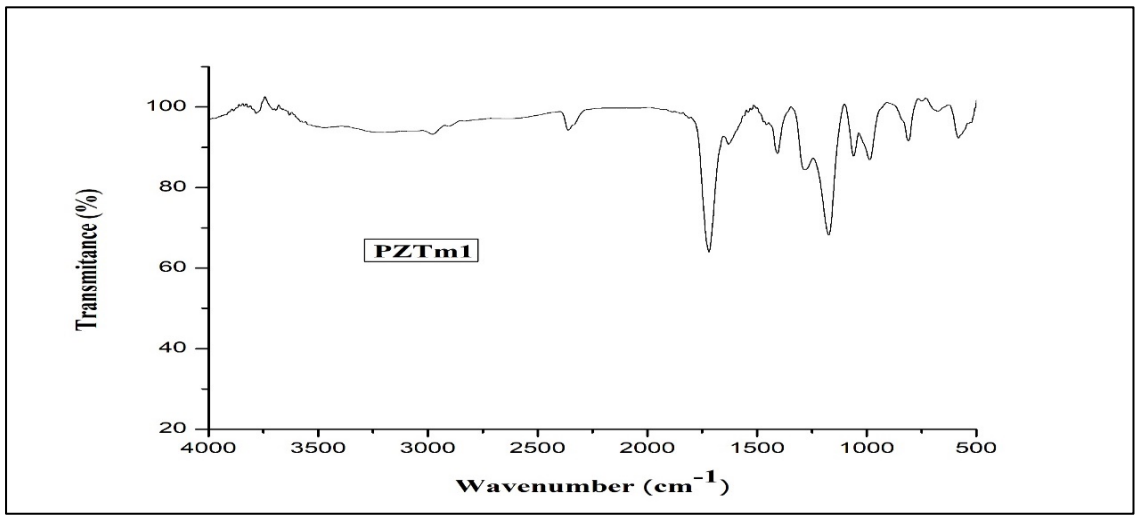

Figure 4.22: FTIR spectra of PZTm1 sample

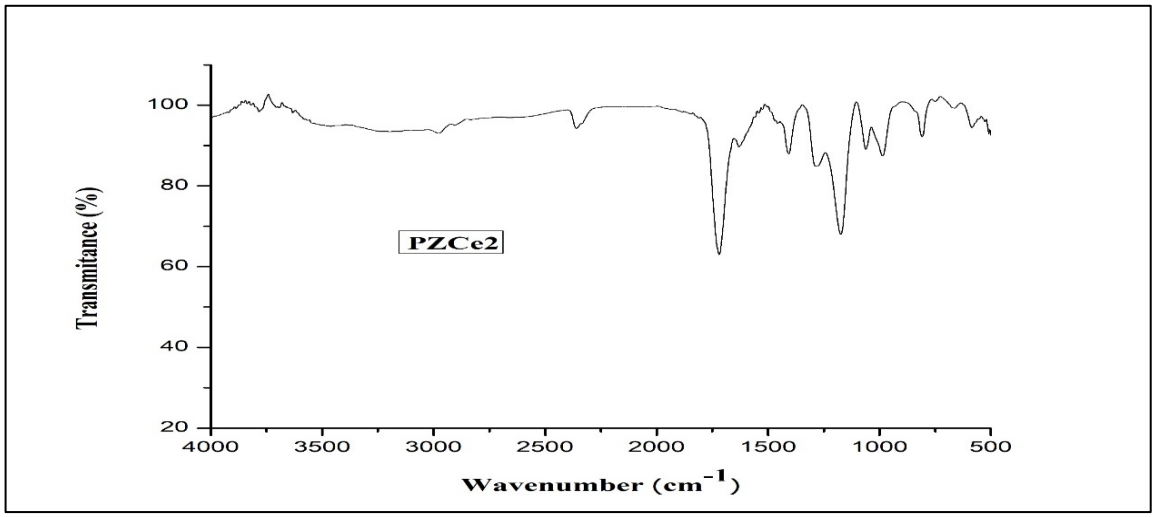

Figure 4.23: FTIR spectra of PZCe2 sample

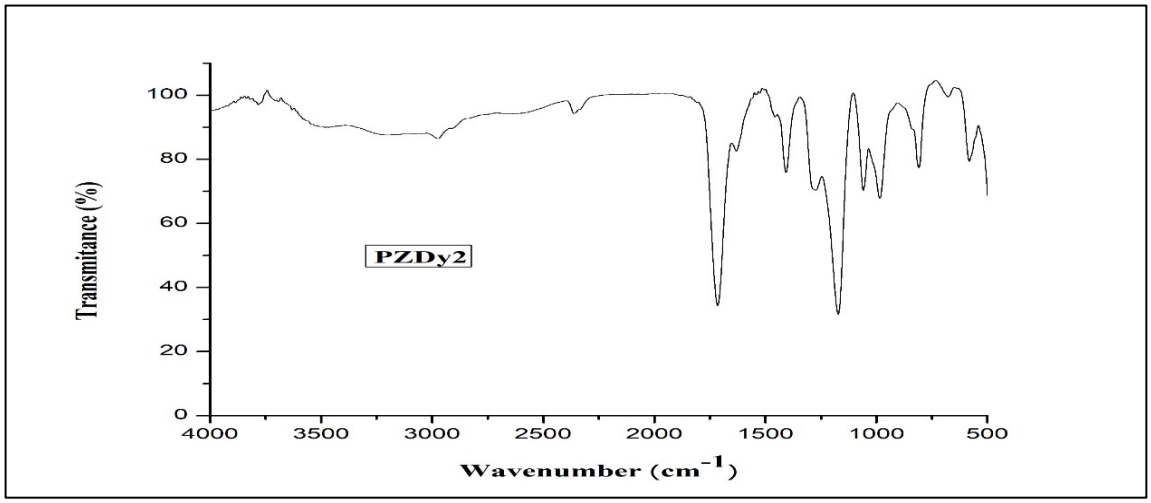

Figure 4.24: FTIR spectra of PZDy2 sample

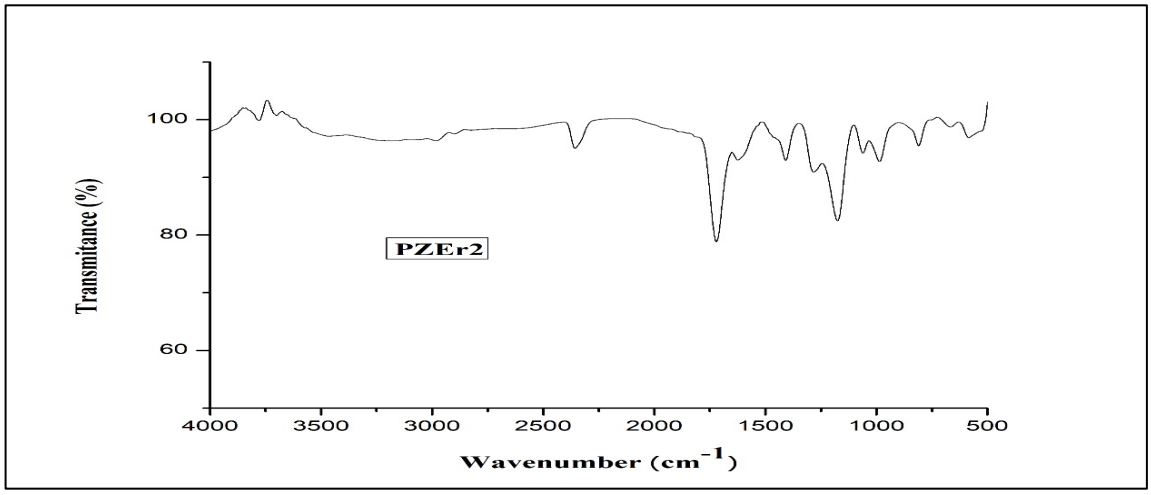

Figure 4.25: FTIR spectra of PZEr2 sample

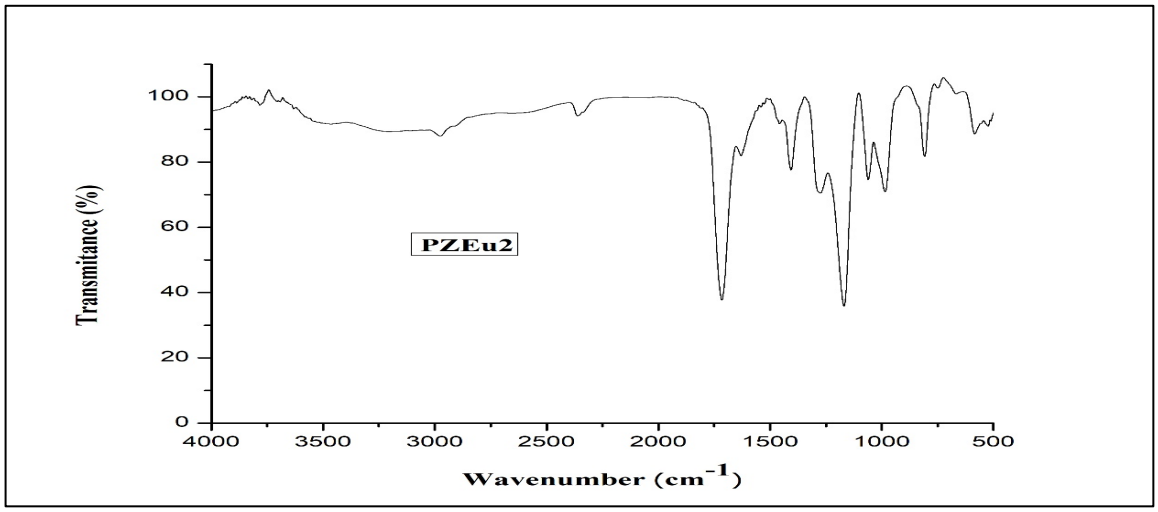

Figure 4.26: FTIR spectra of PZEu2 sample

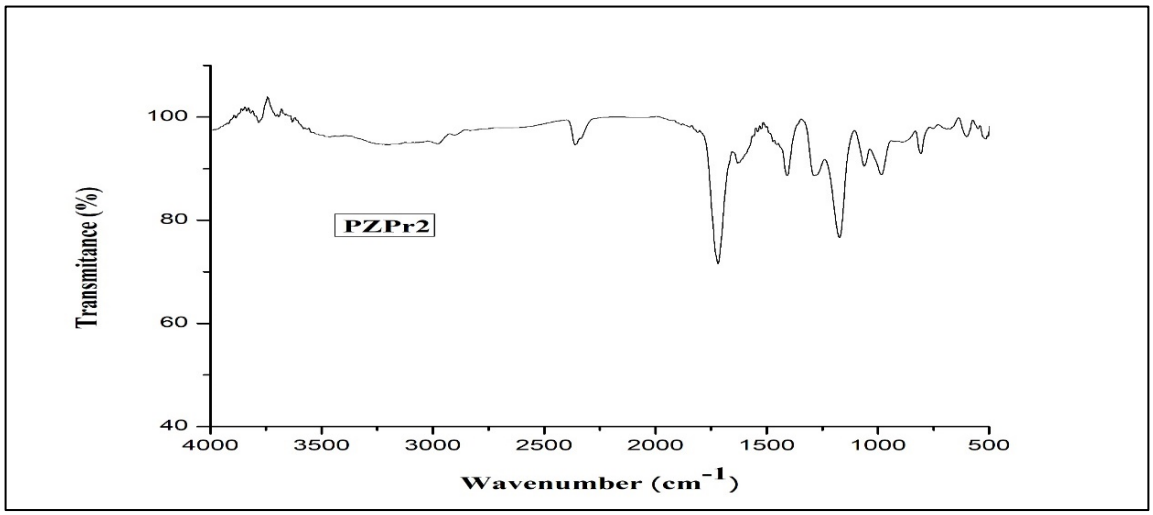

Figure 4.27: FTIR spectra of PZPr2 sample

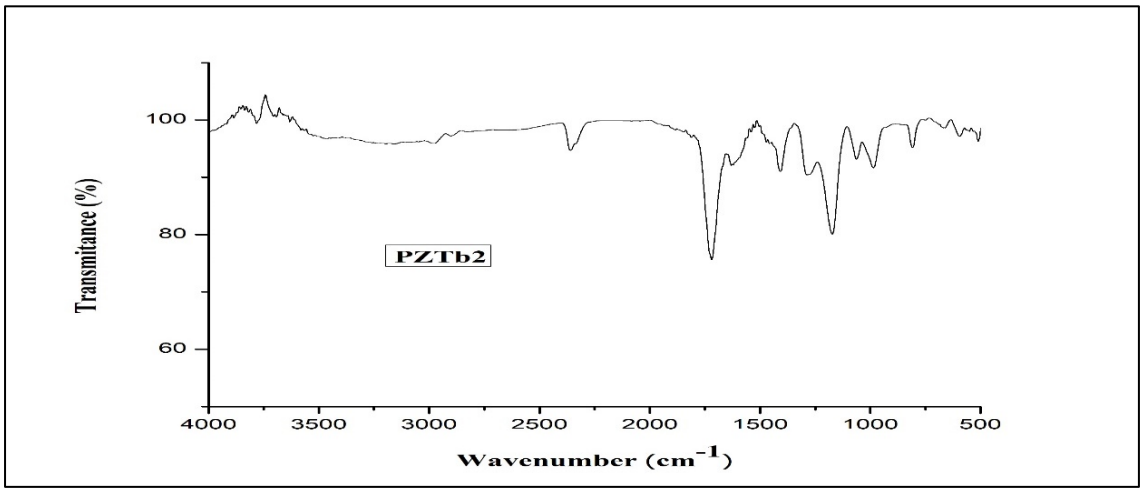

Figure 4.28: FTIR spectra of PZTb2 sample

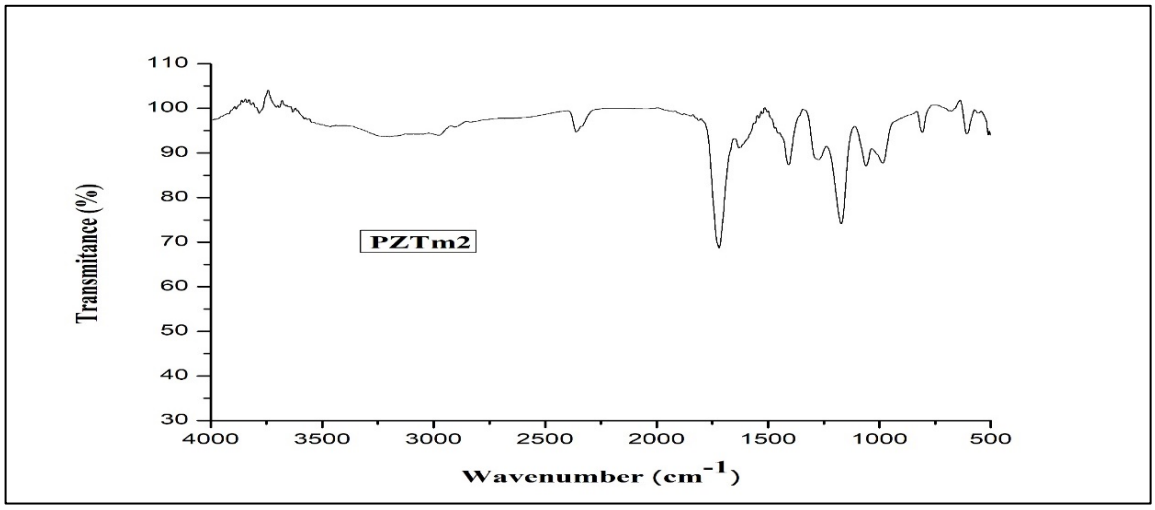

Figure 4.29: FTIR spectra of PZTm2 sample

Table 4.22: Functional group of PAA, PZRE1 and PZRE2 nanocomposites

Wavenumber (cm^{-1})	Functional group
~3500	–OH stretching vibration of water associated with the oxide matrix.
~2970	C–H stretching mode of PAA
~2360	CO_2 linearly adsorbed on the Zr^{4+} ions
~1720	C=O stretching mode of carboxylic group in PAA [3]
~1630	–OH bending mode of hydroxyl groups present on the surface due to moisture
~1460	$–COO^-$ group of PAA [3]
~1405	CH_2 bonding mode of PAA [3]
~1400 and ~590	Zr–O stretching vibrations of ZrO_2 monoclinic phase [4]
~1170	–(C–O)H stretching mode of PAA [3]
~1060	C–CH_2 stretching mode of PAA
~985	various vibrations of the Zr-O bond [4]
~805	CH_2 rocking mode of PAA [3]
Bands at 740	characteristics of tetragonal and monoclinic phases of zirconia
Peaks in the range 500 to 1500	Various Zr–O vibration modes [4]

4.4 Optical Properties:

Study of fluorescence emission of ZrO_2:RE-polyacrylicacid nanocomposites was carried out by Photo-Luminescence (PL) Spectroscopy. UV-Visible Spectroscopy was used to determine the optical properties of the prepared nanocomposites.

4.4.1 Photoluminescence Spectroscopy (PL)

Photoluminescence study was done using JASCO FP-6500 spectrofluorometer. **Figure 4.30** presents the PL spectra of 1 mol% ZrO_2:RE – PAA nanocomposites (PZRE1). The spectra along with that for pure PAA was recorded at 300 nm excitation wavelength. PL spectra of 2 mol% ZrO_2:RE – PAA nanocomposites (PZRE2) and pure PAA recorded at 300 nm excitation wavelength is shown in **Figure 4.31**. The PL spectra exhibits peaks centered at 330 nm in UV emission band and other wide emission peaks centered at 400 nm and 470 nm in the violet-blue emission band, while there is no significant emission in pure PAA at 300 nm excitation.

From **Figure 4.30** and **Figure 4.31**, it can be observed that the overall emission pattern of samples in the UV and violet-blue emission bands remain almost constant. The change occurs only in intensities of PL signals at different wavelength, which can be due to the change in the density of defect levels. The emission peaks are slightly shifted as a function of RE doping percentage.

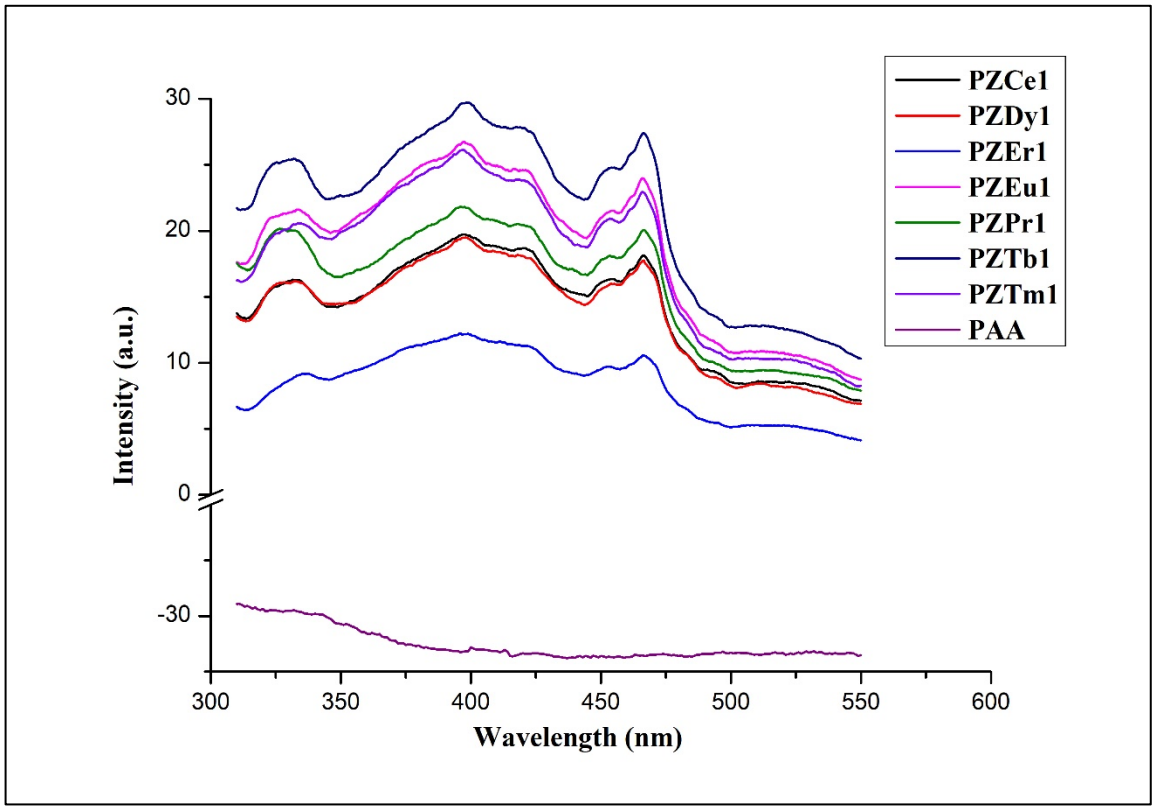

Figure 4.30: PL spectra of PZRE1 (RE= Ce, Dy, Er, Eu, Pr, Tb, Tm) samples

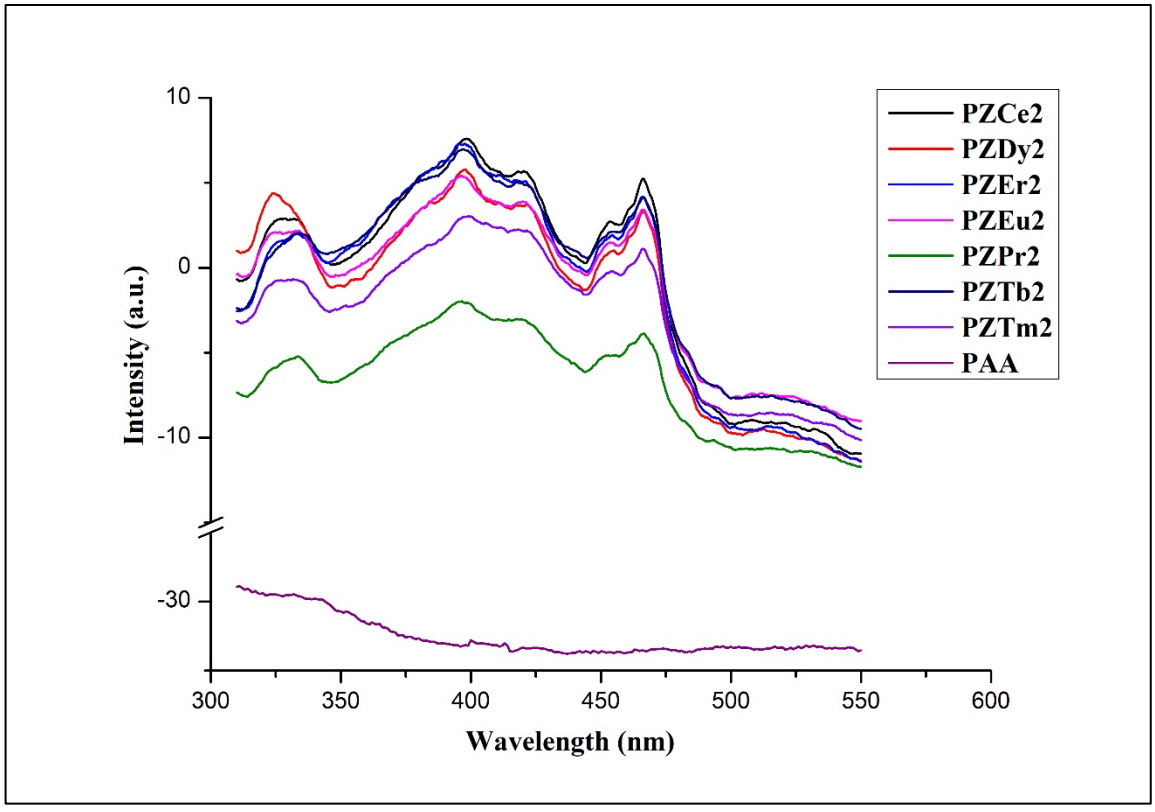

Figure 4.31: PL spectra of PZRE2 (RE= Ce, Dy, Er, Eu, Pr, Tb, Tm) samples

4.4.2 UV-Vis Spectroscopy (UV-Vis)

The optical properties of prepared samples were investigated by UV-Visible absorption spectra. UV-Visible spectroscopic studies were done using UV-3600 Shimadzu spectrometer recorded in the wavelength range 200 to 800 nm. The optical bandgap was evaluated by Tauc's plot. The UV-Visible absorption spectra and corresponding Tauc's plot of pure PAA and 1 mol% ZrO_2:RE – PAA nanocomposites (PZRE1) are shown in **Figures 4.32** to **4.39**. The different optical parameters calculated from UV-Visible absorption spectra are given in **Table 4.23**.

The absorption edge of all the samples lies below 326 nm. The peak absorption wavelengths vary in a range between 272 nm to 292 nm. Hence, there is no substantial change in the absorption pattern.

The optical bandgap of all the RE:ZrO_2-PAA composite samples lie between 3.75 eV to 4.18 eV. The bandgap values of these composite samples are obviously higher compared to pure ZrO_2 which has a band gap of 3.6 eV. The band gap of PAA studied for this work was found to be 4.34 eV. The refractive index of the samples varies in a very short range from 2.12 to 2.20. Eu doped ZrO2 and Dy doped ZrO2 samples show lowest and highest refractive index respectively. This is higher in comparison to reported value of 1.395. The calculated value of refractive index for pure PAA is 2.06.

Figure 4.40 shows variation of absorption coefficient with wavelength. All the samples show higher absorption below 310 nm. After that, the absorption remains constant throughout the visible range. Tm, Tb and Eu doped ZrO_2 samples show relatively higher absorption and found to be decreasing in a pattern given by PZTm1>PZTb1>PZEu1>PZPr1>PZCe1>PZDy1>PZEr1.

Figure 4.41 shows variation of extinction coefficient with wavelength. The value of extinction coefficient remains high for all the samples below 310 nm. The change in extinction co efficient for samples is very small and remains almost uniform throughout the entire range. The values of extinction coefficient rise towards the visible region and near IR. The values are highest for Pr, Dy and Tb doped samples.

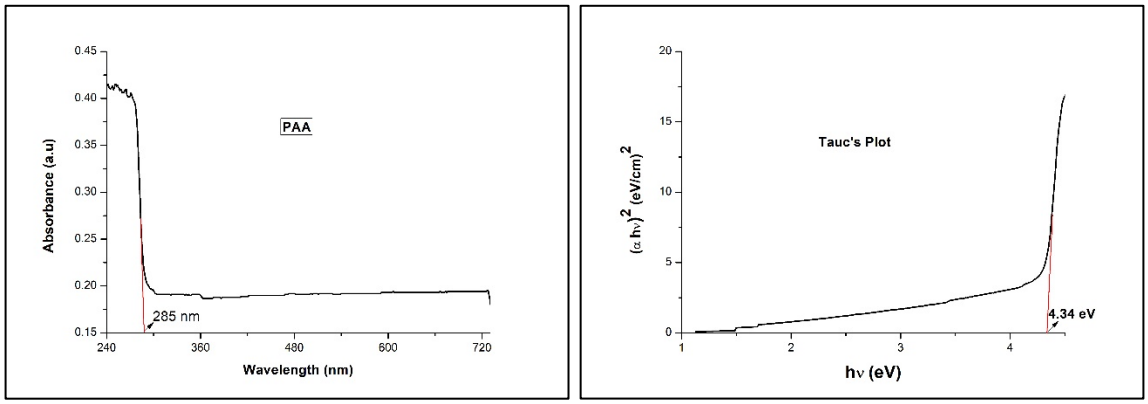

Figure 4.32: UV-Vis absorption spectra and Tauc's plot of pure PAA

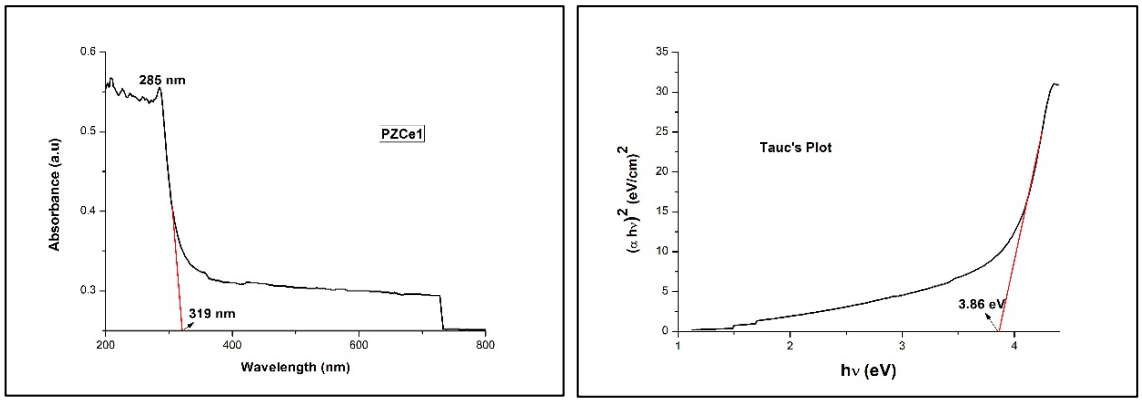

Figure 4.33: UV-Vis absorption spectra and Tauc's plot of PZCe1 sample

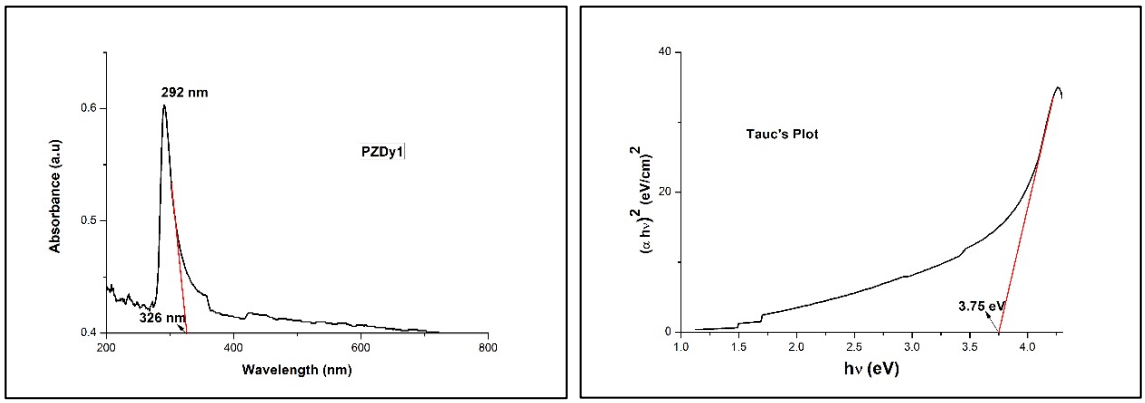

Figure 4.34: UV-Vis absorption spectra and Tauc's plot of PZDy1 sample

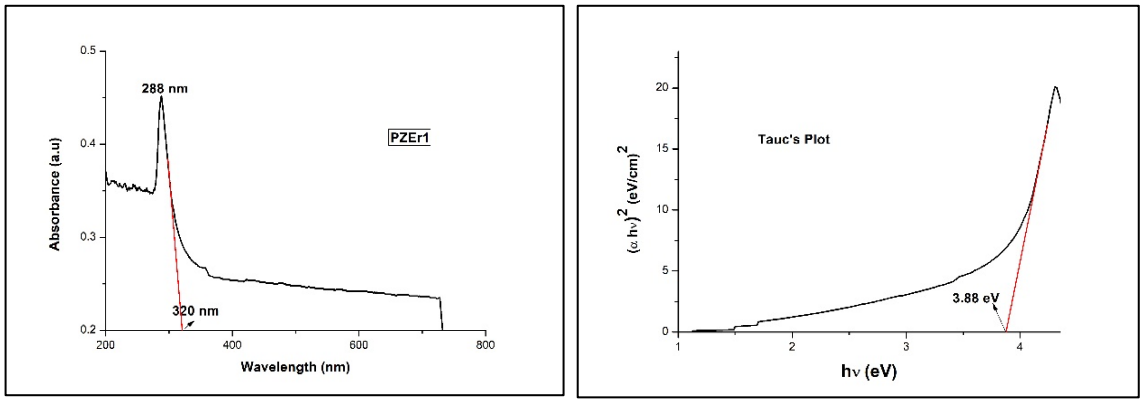

Figure 4.35: UV-Vis absorption spectra and Tauc's plot of PZEr1 sample

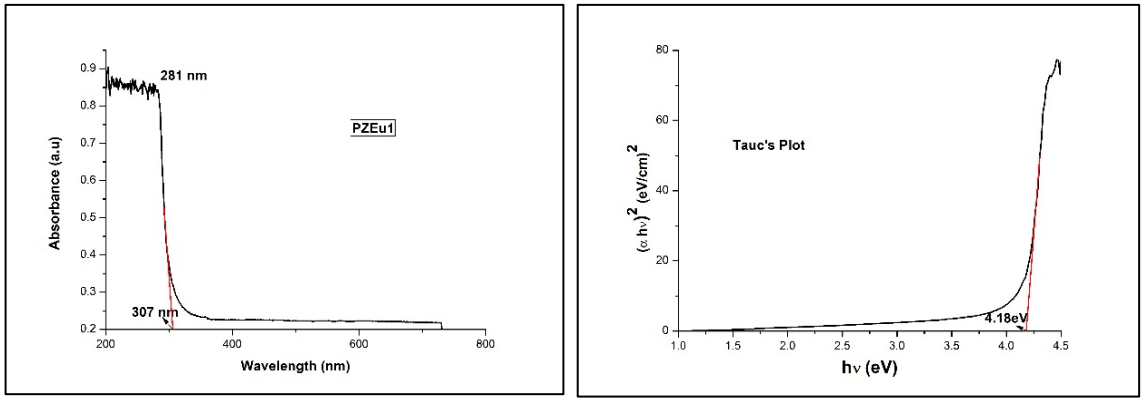

Figure 4.36: UV-Vis absorption spectra and Tauc's plot of PZEu1 sample

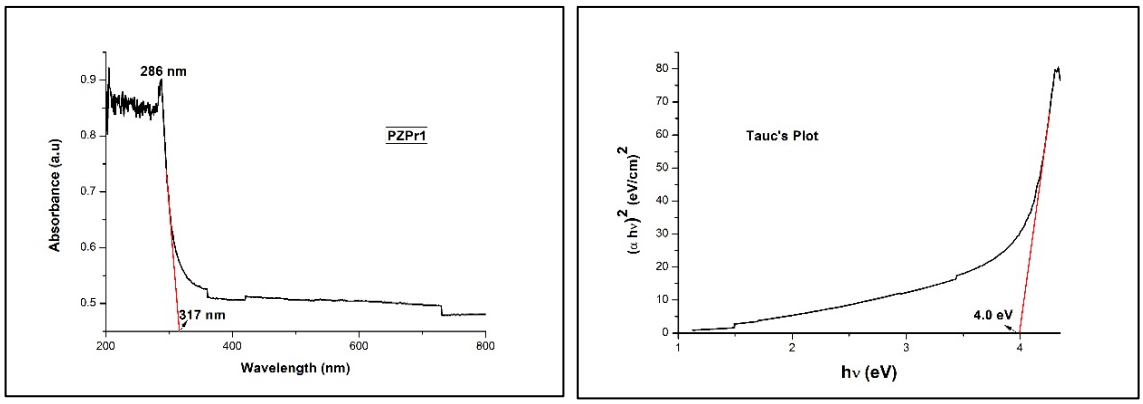

Figure 4.37: UV-Vis absorption spectra and Tauc's plot of PZPr1 sample

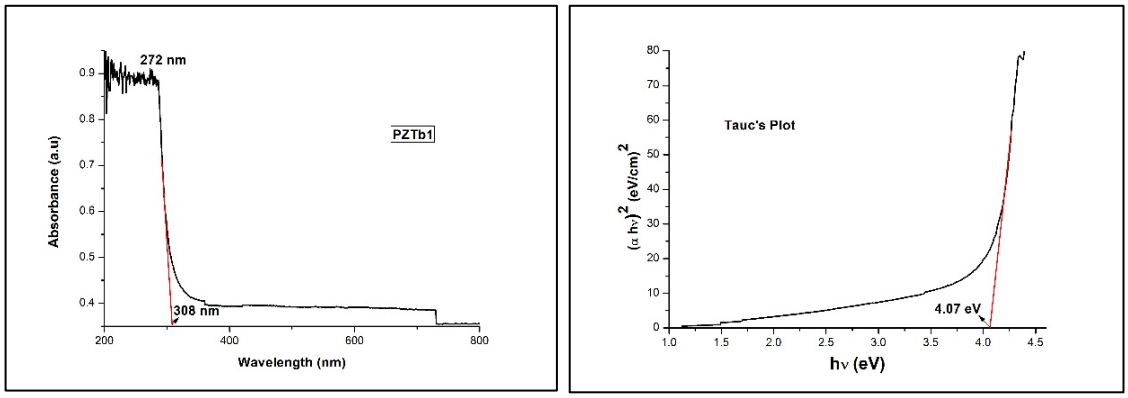

Figure 4.38: UV-Vis absorption spectra and Tauc's plot of PZTb1 sample

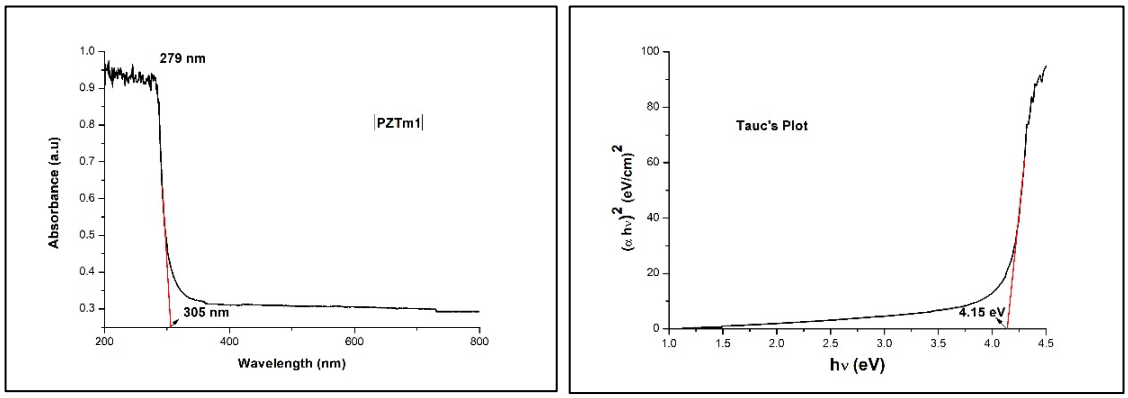

Figure 4.39: UV-Vis absorption spectra and Tauc's plot of PZTm1 sample

Table 4.23: Optical parameters of PZRE1 (RE= Ce, Dy, Er, Eu, Pr, Tb, Tm)

Sample	Peak Absorption	Optical Bandgap	Refractive Index
PAA	285	4.34 eV	2.06
PZCe1	285	3.86 eV	2.18
PZDy1	292	3.75 eV	2.20
PZEr1	288	3.88 eV	2.18
PZEu1	281	4.18 eV	2.12
PZPr1	286	4.00 eV	2.15
PZTb1	272	4.07 eV	2.14
PZTm1	279	4.15 eV	2.13

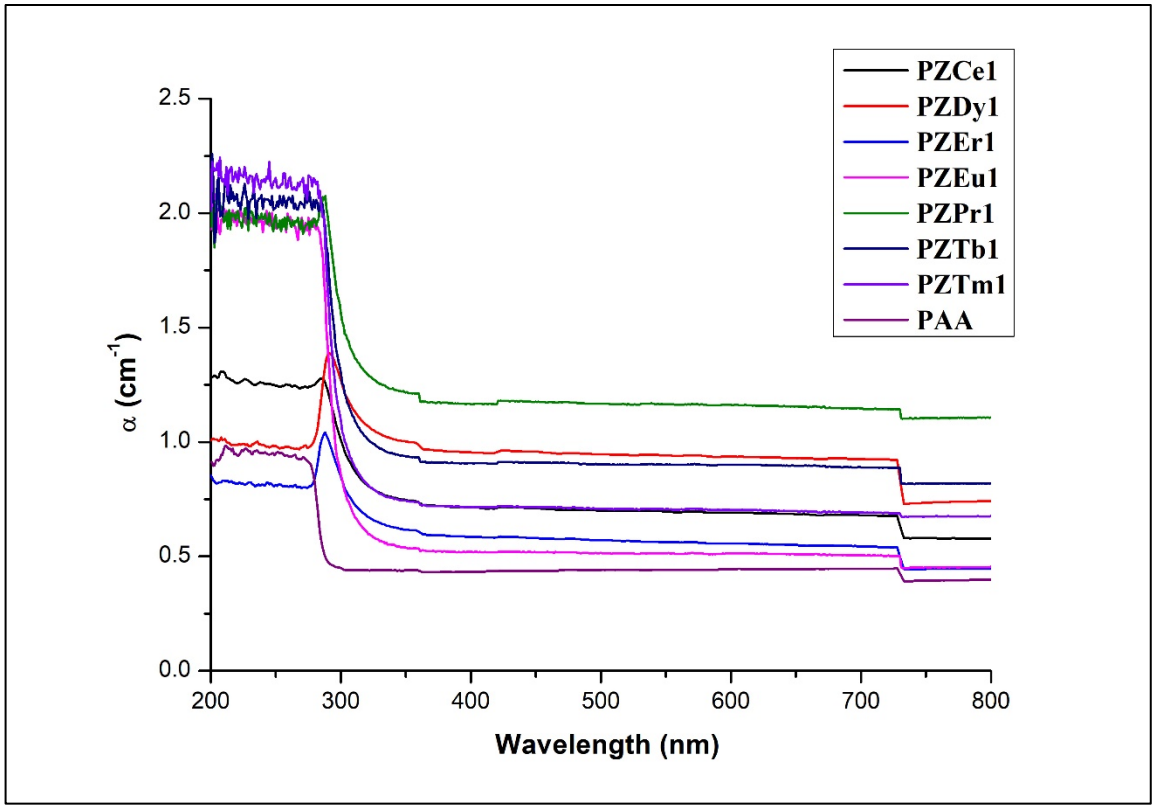

Figure 4.40: Variation of Absorption coefficient with wavelength for PZRE1

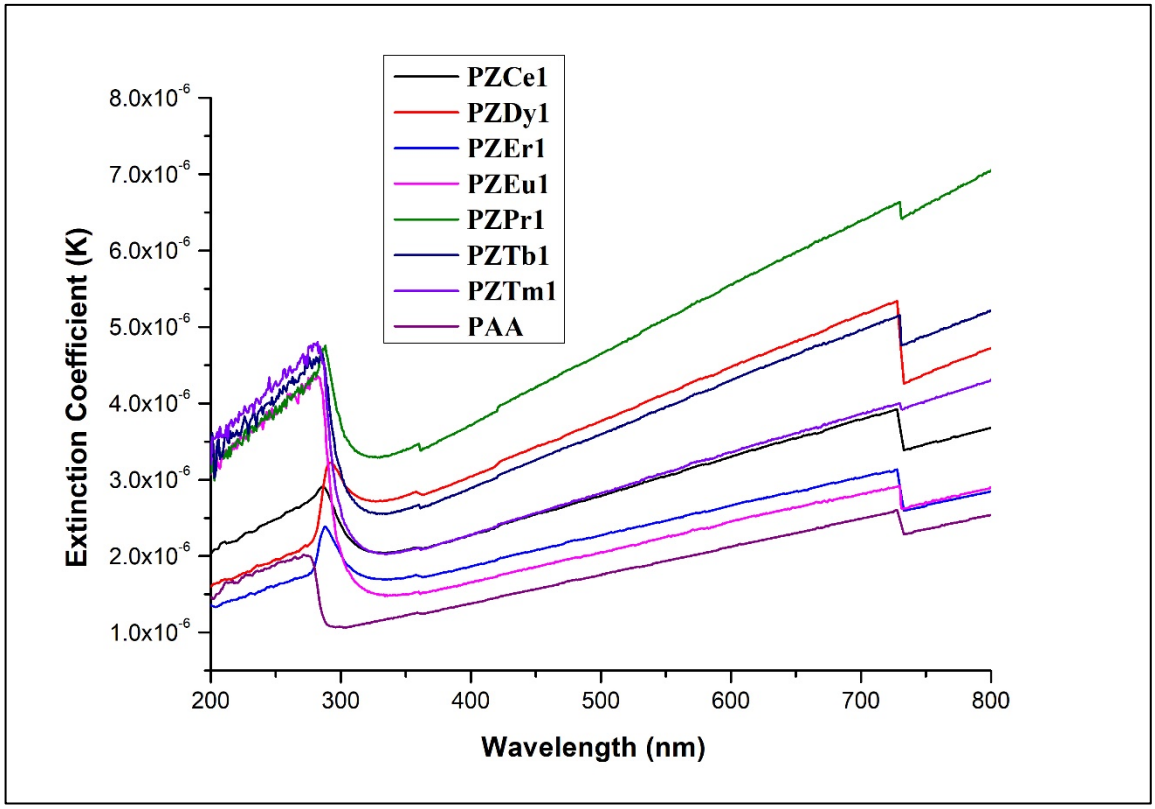

Figure 4.41: Variation of Extinction coefficient with wavelength for PZRE1

The UV-Visible absorption spectra and corresponding Tauc's plot of 2 mol% ZrO2:RE – PAA nanocomposites (PZRE2) shown in **Figures 4.42** to **4.48**. The different optical parameters calculated from UV-Visible absorption spectra are given in **Table 4.24**.

The absorption edge of all the samples lies below 310 nm. The peak absorption wavelengths vary in a range between 272 nm to 292 nm. Hence, there is no substantial change in the absorption pattern. The optical bandgap of all the samples lie between 4.00 eV to 4.25 eV.

The refractive index of the samples vary in a very short range from 2.11 to 2.16. Tm doped ZrO_2 and Dy doped ZrO_2 samples show lowest and highest refractive index respectively.

Figure 4.49 shows variation of absorption coefficient with wavelength. All the samples show higher absorption below 310 nm. After that, the absorption remains constant. Ce, Er and Eu doped ZrO_2 sample shows relatively higher absorption and found to be decreasing in a pattern given by PZCe2>PZEr2>PZEu2>PZPr2>PZTm2>PZTb2>PZDy2. However, it is lower than the samples with 1 mol% blending.

Figure 4.50 shows variation of extinction coefficient with wavelength. The value of extinction coefficient is low for all the samples below 310 nm. The change in extinction co efficient for samples is very small and remains almost uniform throughout the entire range. The values of extinction coefficient rise sharp towards the visible region and near IR. This indicates higher scattering of light in these samples, especially for Dy doped sample.

Hence, PZRE1 set of samples show higher absorption of UV in comparison to PZRE2 samples.

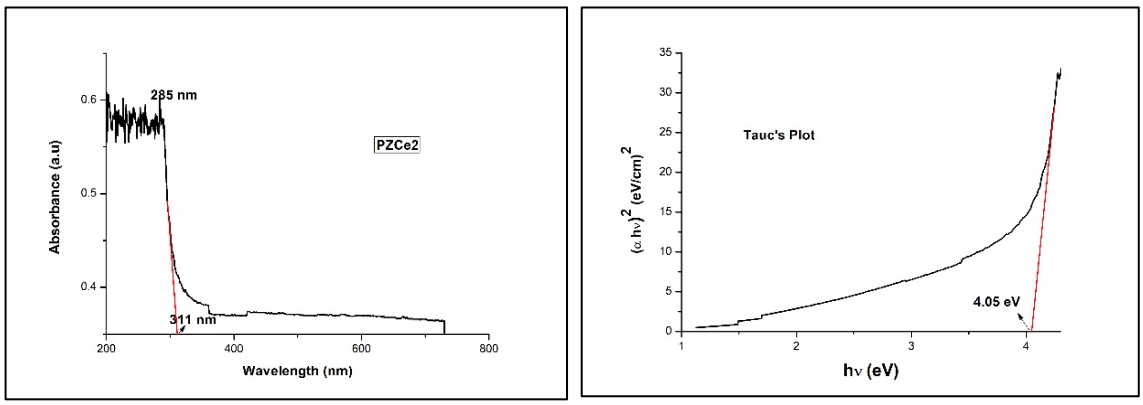

Figure 4.42: UV-Vis absorption spectra and Tauc's plot of PZCe2 sample

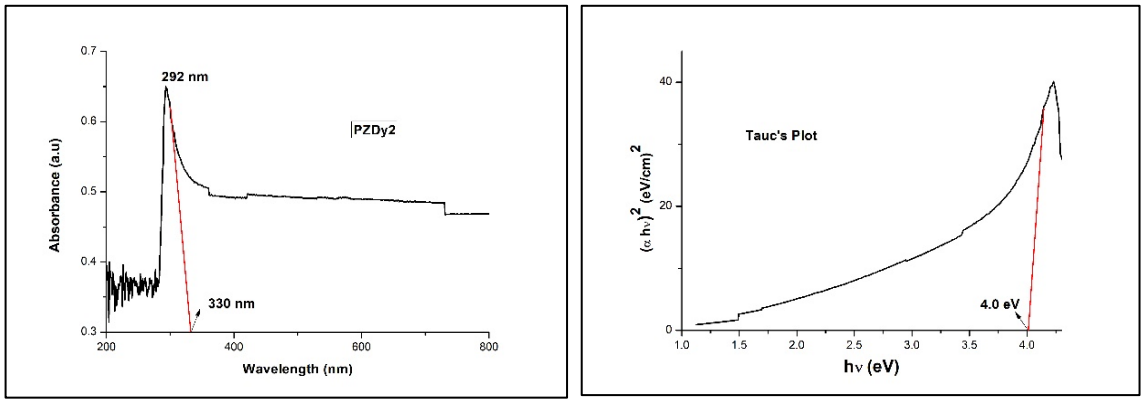

Figure 4.43: UV-Vis absorption spectra and Tauc's plot of PZDy2 sample

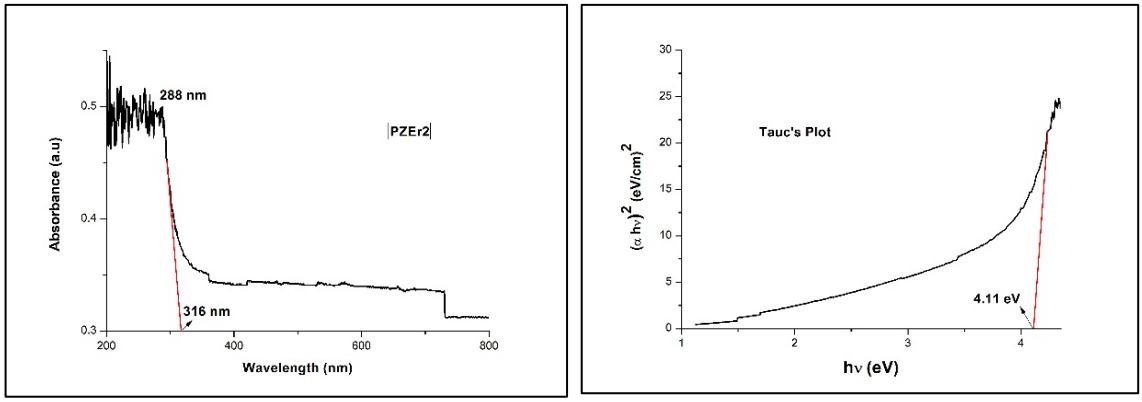

Figure 4.44: UV-Vis absorption spectra and Tauc's plot of PZEr2 sample

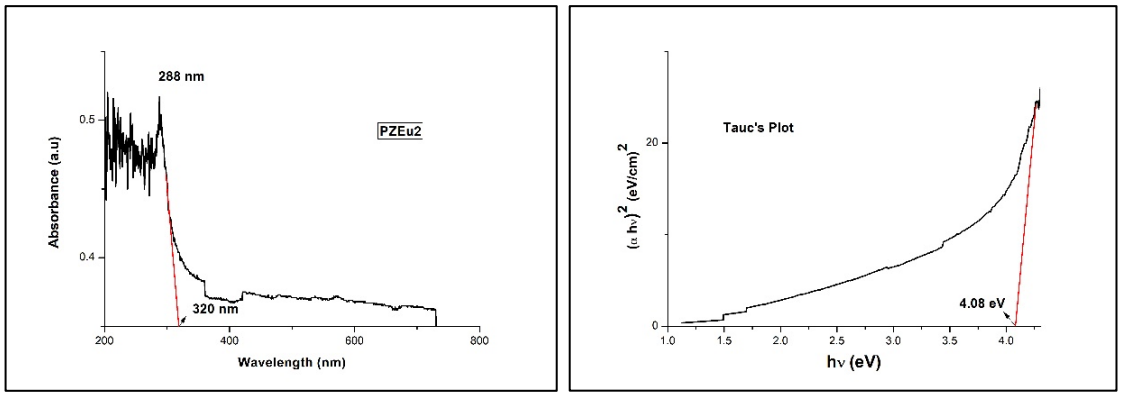

Figure 4.45: UV-Vis absorption spectra and Tauc's plot of PZEu2 sample

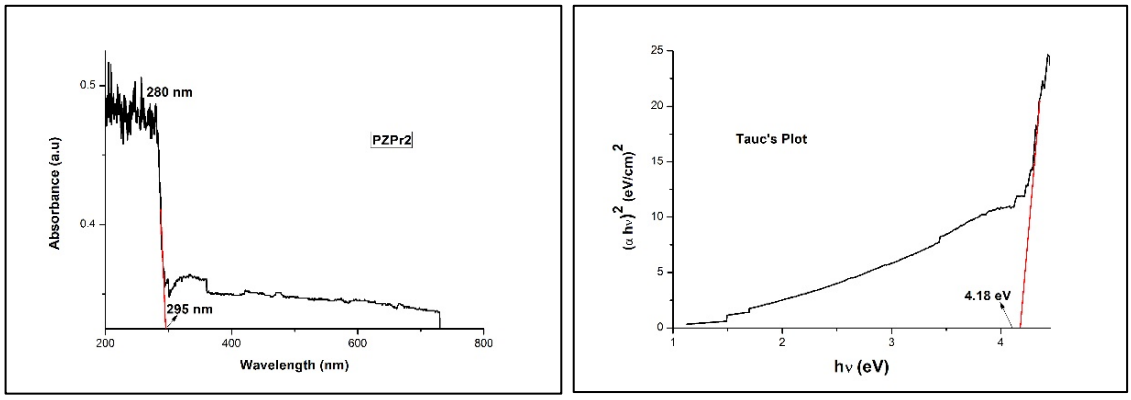

Figure 4.46: UV-Vis absorption spectra and Tauc's plot of PZPr2 sample

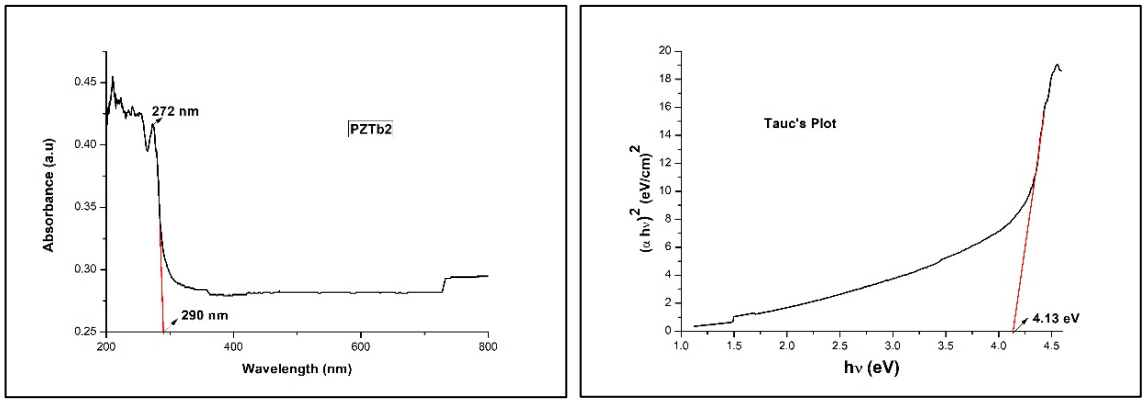

Figure 4.47: UV-Vis absorption spectra and Tauc's plot of PZTb2 sample

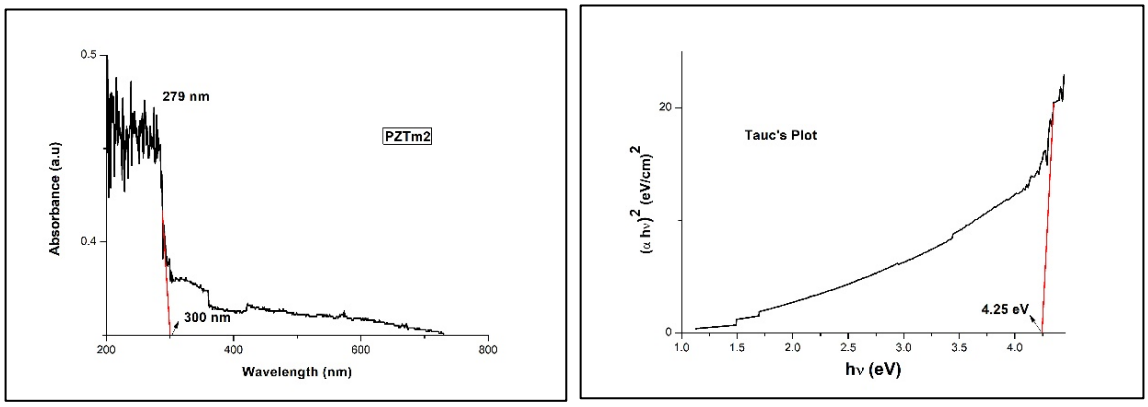

Figure 4.48: UV-Vis absorption spectra and Tauc's plot of PZTm2 sample

Table 4.24: Optical parameters of PZRE2 (RE= Ce, Dy, Er, Eu, Pr, Tb, Tm)

Sample	Peak Absorption	Optical Bandgap	Refractive Index
PAA	285	4.34 eV	2.06
PZCe2	285	4.05 eV	2.15
PZDy2	292	4.00 eV	2.16
PZEr2	288	4.11 eV	2.14
PZEu2	288	4.08 eV	2.14
PZPr2	280	4.18 eV	2.12
PZTb2	272	4.13 eV	2.13
PZTm2	279	4.25 eV	2.11

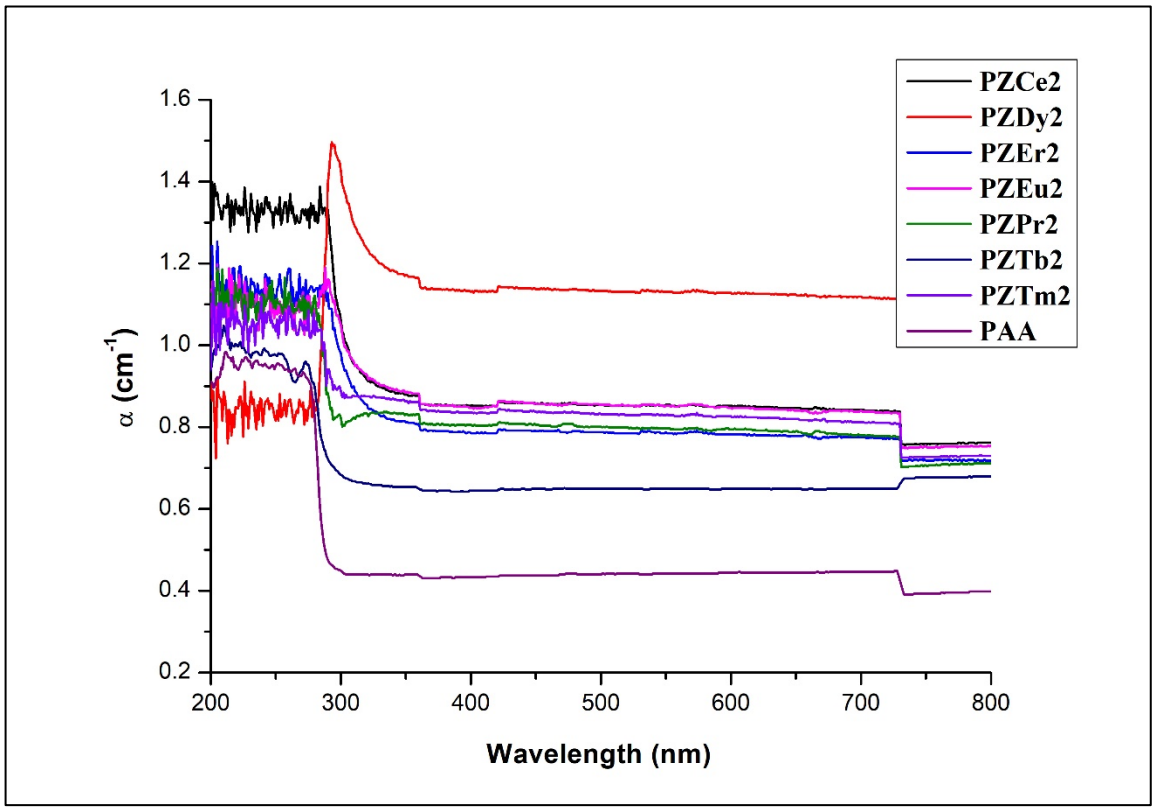

Figure 4.49: Variation of Absorption coefficient with wavelength for PZRE2

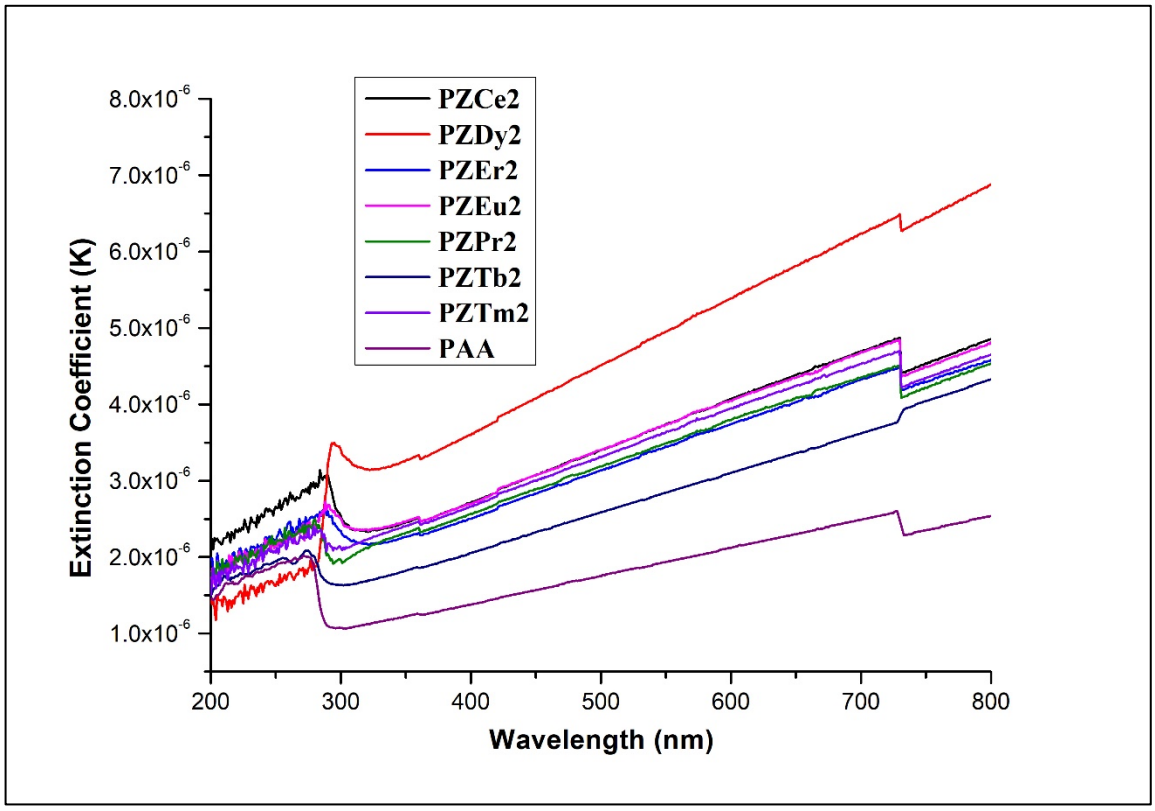

Figure 4.50: Variation of Extinction coefficient with wavelength for PZRE2

4.5 Summary:

Rare earth doped ZrO_2 – PAA nanocomposites were prepared using hydrothermal method and doctor blade method. The XRD results revealed the formation of material as nano crystallite and confirms the material structure formation and it matches with the standard JCPDS results. DLS results give particle size distribution in nano meters. The EDS spectra of samples indicates the presence of Zirconium, Oxygen and rare earth elements. The FTIR spectra confirms the presence of different functional groups with respective wavenumber for PAA. The Photoluminescence study exhibits wide peaks in UV region and violet-blue region.

The optical properties of material were analysed by UV- Visible Spectroscopy. The bandgap values of the composites are between that of pure ZrO_2 and pure PAA. The refractive index is higher than pure PAA. The variation of absorption coefficient with wavelength shows higher absorption in UV range. The value of extinction coefficient is high for all the samples below 310 nm. The results of the optical studies are correlated and can be used for its possible applications. PZRE1 (1 mol%) set of samples show higher absorption of UV in comparison with PZRE2 (2 mol%) samples.

References:

[1] A. L. Patterson, "The Scherrer Formula for X-Ray Particle Size Determination", Phys. Rev., 56 (1939), pp. 978

[2] JCPDS-ICDD, Joint committee for powder diffraction standards, International Center of Diffraction Data (1997).

[3] Chiam-Wen Liew, H.M. Ng, Arshid Numan, S. Ramesh, Poly(Acrylic acid)–Based Hybrid Inorganic–Organic Electrolytes Membrane for Electrical Double Layer Capacitors Application, Polymers 8, 179 (2016).

[4] Elaheh K. Goharshadi, Mahboobeh Hadadian, Effect of calcination temperature on structural, vibrational, optical, and rheological properties of zirconia nanoparticles, Ceramics International 38 (2012) 1771–1777.